



# Design of pre-stressed plate-strips to cover non-developable shells

Alexandre Danescu, Ioan Ionescu

## ► To cite this version:

Alexandre Danescu, Ioan Ionescu. Design of pre-stressed plate-strips to cover non-developable shells. European Journal of Mechanics - A/Solids, 2022, 95, pp.104609. 10.1016/j.euromechsol.2022.104609 . hal-03866677

**HAL Id: hal-03866677**

**<https://hal.science/hal-03866677>**

Submitted on 26 Jan 2024

**HAL** is a multi-disciplinary open access archive for the deposit and dissemination of scientific research documents, whether they are published or not. The documents may come from teaching and research institutions in France or abroad, or from public or private research centers.

L'archive ouverte pluridisciplinaire **HAL**, est destinée au dépôt et à la diffusion de documents scientifiques de niveau recherche, publiés ou non, émanant des établissements d'enseignement et de recherche français ou étrangers, des laboratoires publics ou privés.

# Design of pre-stressed plate-strips to cover non-developable shells

Alexandre Danescu\* and Ioan R. Ionescu†

version : January 27, 2022

## Abstract

In this paper we address the following design problem: what is the shape of a plate and the associated pre-stress that relaxes toward a given three-dimensional shell ? As isometric transformations conserve the gaussian curvature, three-dimensional non-developable shells cannot be obtained from the relaxation of pre-strained plates by using isometric transformations only. Overcoming this geometric restriction, including small-strains and large rotations, solves the problem for small areas only. This paper dispenses with the small-area restriction to cover three-dimensional shells fully by using shell-strips. Since shell-strips have an additional geometric parameter, we show that under suitable assumptions that relate the width of the strip to the curvature of the shell, we are able to design arbitrary shell surfaces by covering them with shell-strips. As an illustration, we provide optimized covers of the sphere in a variety of different surface-strips relaxed from plate-strips with homogeneous and isotropic pre-stress. Moreover, we propose the design of the torus, of the helicoid and of the non-developable Möbius band, which requires inhomogeneous and anisotropic pre-stress.

**Keywords:** nonlinear elasticity, large rotations and small strains, shell design, pre-stress, non-developable strip-surfaces.

---

\*University of Lyon, Institute of Nanotechnologies - INL, UMR CNRS 5270, Ecole Centrale de Lyon, Ecully, France, [alexandre.danescu@ec-lyon.fr](mailto:alexandre.danescu@ec-lyon.fr)

†LSPM, University Sorbonne-Paris-Nord, Villetaneuse, France, and IMAR, Romanian Academy, Bucharest, Romania, [ioan.r.ionescu@gmail.com](mailto:ioan.r.ionescu@gmail.com)

# Contents

<b>1</b>	<b>Introduction</b>	<b>2</b>
<b>2</b>	<b>Plate-to-shell equations for design</b>	<b>5</b>
2.1	Geometric assumptions . . . . .	5
2.2	Constitutive assumptions . . . . .	6
2.3	Moment plate-to-shell equations . . . . .	8
<b>3</b>	<b>Designing a pre-stressed plate-strip for a given shell-strip</b>	<b>9</b>
3.1	Designing strips with small strain . . . . .	9
3.1.1	Constructing a second-order strip along a curve on a surface . . .	9
3.1.2	Lagrangian planar strip . . . . .	11
3.1.3	Mapping a planar-strip into a surface-strip . . . . .	11
3.1.4	Designing the planar strip . . . . .	13
3.2	Designing the plate-strip for a given shell-strip . . . . .	13
<b>4</b>	<b>Applctions to non-developable shells</b>	<b>14</b>
4.1	Strips on spherical surfaces . . . . .	15
4.1.1	"Orange-peeling" strips . . . . .	16
4.1.2	Covering a sphere with meridian strips . . . . .	16
4.1.3	Covering a sphere with parallel strips . . . . .	18
4.2	Strips on a torus . . . . .	19
4.3	Rotoidal strips . . . . .	22
4.3.1	Helicoid . . . . .	23
4.3.2	Classical Möbius ribbon . . . . .	24
<b>5</b>	<b>Conclusions and perspectives</b>	<b>26</b>
<b>6</b>	<b>Appendix</b>	<b>31</b>

## 1 Introduction

Modern technological developments for semiconductors at the nanoscale, such as Molecular Beam Epitaxy (MBE), allow very fine tuning of the material properties through control of the lattice parameter, while the geometry of the domain can be easily implemented by using photolithography. However, the lattice mismatch between the planar

template and the grown crystal should be kept as small as possible and the fabrication technology at the nano-scale is essentially planar. But from a practical point of view, the bending process of a pre-stressed multi-layer material may be beneficial, as one can use it to design various three-dimensional objects starting from planar pre-strained templates, thus encompassing the planar technology.

Since the semiconductors are anisotropic elastic/brittle materials, the study of the equilibrium shape for a bilayer plate of a given geometry can be formulated as a classical linear or nonlinear direct elasticity problem. Given either a specific or a generic elastic energy, one looks for the existence/uniqueness/approximation of configurations that realizes the local (or global) minimum of the considered elastic energy. For the modeling aspects in thin layer pre-stressed materials, asymptotic models inspired by dimension reduction were proposed in [1, 2, 3, 4, 5, 6, 7, 8]. The linear approach cannot recover experimental results illustrated, for instance, in [9] for the relaxed configurations that do not fit the small perturbation theory, which is a situation frequently encountered in applications. This is a benchmark for various asymptotic and/or exact nonlinear models for elastic plates/shells, and recent results [10, 11] on various approximations of the three-dimensional elasticity with incompatible pre-strain/stress provide a hierarchy of non-linear elastic models.

However, the classical approach cannot answer the following important practical question: *what is the two-dimensional shape that relaxes toward a given three-dimensional surface/object?* For problems of design by stress relief for a given target geometry, we are looking for an elastic, pre-stressed material and a reference geometry so that the target geometry represents the naturally relaxed configuration of the reference geometry. The minimal mechanical and geometrical setting needed to address the general design problem mentioned above is that of small strains but large rotations. The motivation of the small strains assumption relies mainly on the fact that the single source of elastic energy is the small pre-strain/pre-stress, while the large rotations framework is needed, since in most situations the planar design contains a large characteristic length. Moreover, since we are focusing on brittle-elastic materials (such as semiconductors), the small deformations assumption is merely a *technological restriction* and not a mathematical simplification.

Previous results [9, 12, 13, 14, 15, 16] concerning relaxation of pre-stressed bilayer materials focus on straight ribbons that relax toward rolls and curls, all based on isometric transformations. However, it is well-known that the class of isometries between planar and three-dimensional surfaces, extensively studied in [17], is too narrow to cover simple non-developable surfaces occurring in pre-stressed relaxation design problems. To circumvent



this theoretical drawback, in a recent paper [18] we developed a shell design model built on a non-isometrical perturbation assumption (of Love-Kirchhoff type superposed on a plate-to-shell theory [19, 20, 21, 22, 23]). The geometric description involves a single small parameter  $\delta \ll 1$ , the product between the thickness of the shell and its curvature.

The main difficulty in applying a shell design model [18] is of a geometric nature. Indeed, for several common mid-surfaces the small-strain assumption drastically reduces the surface width. For instance, only small parts of a spherical shell can be recovered from the pre-stressed plates as shown in Fig. 4 in [18]. To encompass this limitation, in this paper we construct another type of shell, called a strip-shell, for which this assumption can be fulfilled by an appropriate choice of an additional geometric parameter, namely the strip width. The geometries of shell-strips introduce an additional small parameter, further denoted  $\eta$ , which is the ratio between the width of the strip and the curvature radius. Then, for  $\delta = \eta^2$  the assumptions of plate-to-shell theory [18] are fulfilled and for any strip of a given shell we obtain a simple model to design the corresponding plate-strip (i.e., to compute the shape and pre-stress moment of the plate). The next step is to cover the given surface (shell) with one or several strips, for which we can design the corresponding planar (plate) strips.

The design problem we address here was also previously considered in [24, 25, 26, 27] in a different context where the in-plane average pre-stress related to growth was considered in contrast to our thickness variation approach suitable for planar fabrication technology.

This paper is structured as follows: the second section presents the basic geometric, kinematic and constitutive assumptions and a simplified version of the plate-to-shell model for the design obtained in [18]. The third section addresses the particular problem of the design for a shell-strip from a pre-stressed plate-strip. As previously mentioned, by requiring the ratio between the shell-strip thickness and the shell-strip width to be  $\mathcal{O}(\sqrt{\delta})$ , we can use the shell-to-plate theory to obtain the pre-stress bending moment. More exactly, we define a second-order strip constructed along an arbitrary curve of the shell mid-surface and its Lagrangian counterparts, a planar strip along a planar curve. We prove that the natural mapping of the plate-strip to a shell-strip is a small strain transformation if the curvature of the planar strip coincides with the geodesic curvature of the shell-strip and some other additional conditions on the width are fulfilled. The design problem we address includes much more than the class of isometric transformation so that, under specific assumptions, we are able to design shells for which the Gaussian curvature of the mid-surface does not vanish. The fourth section offers three examples in this class: three designs that completely cover the sphere, two designs that partially

cover the torus and, finally, two examples of rotoidal strips (helicoid and classical Möbius ribbon).

## 2 Plate-to-shell equations for design

In this section, we present a simplified version of the model obtained in [18] for plate-to-shell design. In the applications we have in mind, the pre-stress/strain has an important thickness heterogeneity but the material properties are almost homogeneous. Here, this allows us to consider only materials with a weak transversal material heterogeneity. In this case, an important simplification of the model appears: the six equations for the design problem can be decoupled in two families. Three of them involve the small perturbation which can be computed from the membrane deformation and the pre-stress resultant, and will not be used in the design problem. The remaining three, also called the design equations, involve the three components of the pre-stress moments and the membrane curvature.

### 2.1 Geometric assumptions

Let  $\mathbf{s}_0 \subset \mathbb{R}^3$  be the design Eulerian mid-surface and let  $\mathbf{e}_3$  denote the unit normal, and  $\mathcal{K}$  the curvature tensor acting from the tangent plane  $\mathcal{T}$  into itself. The designed shell is the given by

$$\mathbf{s} = \{\mathbf{x}_0 + x_3 \mathbf{e}_3(\mathbf{x}_0) ; \mathbf{x}_0 \in \mathbf{s}_0, x_3 \in (-\frac{h}{2}, \frac{h}{2})\}, \quad (2.1)$$

where  $h = h(\mathbf{x}_0)$  is the shell thickness. Let us also consider that

$$\mathcal{S} = \{X = (\bar{X}, X_3); \bar{X} \in \mathcal{S}_0, X_3 \in (-\frac{H(\bar{X})}{2}, \frac{H(\bar{X})}{2})\} \quad (2.2)$$

is the Lagrangian plate with mid-surface  $\mathcal{S}_0 \subset \mathbb{R}^2$  and thickness  $H = H(\bar{X})$  in the Lagrangian configuration, where we use  $\bar{X} = (X_1, X_2)$ .

In what follows,  $\delta \ll 1$  will be a small parameter characterizing the Eulerian and Lagrangian shell thickness through

$$h|\mathcal{K}| = \mathcal{O}(\delta), \quad \frac{H}{L_c} = \mathcal{O}(\delta), \quad |\nabla_2 H| = \mathcal{O}(\delta), \quad (2.3)$$

where  $L_c$  is the characteristic length of the surface and  $\nabla_2$  is the gradient with respect to  $\bar{X} \in \mathcal{S}_0$ .

The *main geometric assumption* is that there exists a transformation  $\mathbf{x}_0 : \mathcal{S}_0 \rightarrow \mathbb{R}^3$

of the Lagrangian mid-surface  $\mathcal{S}_0$  into the designed Eulerian one  $\mathbf{s}_0$  (i.e.,  $\mathbf{s}_0 = \mathbf{x}_0(\mathcal{S}_0)$ ) such that the associated deformation of the geometric transformation is small, i.e.,

$$|\mathbf{F}_0^T(\bar{X})\mathbf{F}_0(\bar{X}) - \mathbf{I}_2| = \mathcal{O}(\delta), \quad \text{for all } \bar{X} \in \mathcal{S}_0. \quad (2.4)$$

Here,  $\mathbf{F}_0 = \nabla_2 \mathbf{x}_0$  is the gradient tensor acting in each point  $\bar{X} = (X_1, X_2) \in \mathcal{S}_0$ , from  $\mathbb{R}^2$  into the tangent plane  $\mathcal{T}(\mathbf{x}_0(\bar{X}))$  of the designed surface  $\mathbf{s}_0$  and  $\mathbf{I}_2 = \mathbf{c}_1 \otimes \mathbf{c}_1 + \mathbf{c}_2 \otimes \mathbf{c}_2$  is the identity tensor on  $\mathbb{R}^2$  and  $\{\mathbf{c}_1, \mathbf{c}_2, \mathbf{c}_3\}$  is the Cartesian basis in the Lagrangian description. We further denote by  $\mathbf{K} = \mathbf{F}_0^T \mathcal{K} \mathbf{F}_0$  the Lagrangian curvature tensor acting from  $\mathbb{R}^2$  into itself.

The kinematics of the plate deformation involves the classical Love-Kirchhoff assumption, i.e.: *the normal to the plate mid-plane remains normal to the designed mid-surface* but in a finite deformation context and thus including large rotations. In addition, the transversal deformation is affine with respect to the plate thickness. Superposed to the kinematics associated to the exact design which reproduces the target mid-surface, we consider a small perturbation of Love-Kirchhoff type in order to compensate the small (membrane) deformation of the proposed geometric transformation. As a consequence, the mid-surface of this overall kinematics will be close to the designed mid-surface, and for this reason we called it *approximative designed kinematics*. Our main goal is to provide conditions which ensure that an approximative designed configuration can be reached by releasing a suitable pre-strained plate.

## 2.2 Constitutive assumptions

From the constitutive point of view, applications to semiconductor materials require cubic materials under bi-axial pre-strain. We also assume weak transverse material heterogeneity that ensures the decoupling between average and moment equations. This significant simplification of the proposed model is motivated by the fact that, in most of the applications to semiconductor layers grown by MBE, the pre-strain is induced by the fine-tuning of the layers composition (for instance  $\text{In}_{1-\alpha}\text{Ga}_\alpha\text{P}$  for small  $\alpha$ ). With these ingredients, we were able to rely on the theoretical predictions with the experimental evidence [28, 29] for thin ( $\simeq 200$  nm thick) semiconductor pre-strained multi-layers.

Here we consider a pre-stressed hyper-elastic material undergoing small strains but large rotations. If  $|\mathbf{E}| = \mathcal{O}(\delta)$  is the strain tensor and  $\mathbf{S}$  is the second Piola-Kirchhoff

stress tensor, then the constitutive equation reads

$$\mathbf{S} = \mathbf{C}\mathbf{E} + \mathbf{S}^* + \Sigma\mathcal{O}(\delta^2), \quad (2.5)$$

where  $\mathbf{C}$  is the fourth-order tensor of elastic coefficients and  $\mathbf{S}^* = \mathbf{S}^*(\bar{X}, X_3)$  is the pre-stress with  $|\mathbf{S}^*| = \Sigma\mathcal{O}(\delta)$  and  $\Sigma$  is a characteristic stress.

In what follows, we consider only orthotropic materials with the elastic coefficients (Voigt notation)  $C_{ij} = C_{ij}(\bar{X}, X_3)$ , i.e.,

$$\mathbf{C}\mathbf{A} = \mathbf{C}_2\mathbf{A}_2 + A_{33}\mathbf{C}_3 + (\mathbf{C}_3 : \mathbf{A}_2 + C_{33}A_{33})\mathbf{c}_3 \otimes \mathbf{c}_3 + 4C_{44}A_{23}(\mathbf{c}_2 \otimes \mathbf{c}_3)_S + 4C_{55}A_{13}(\mathbf{c}_1 \otimes \mathbf{c}_3)_S,$$

where we have denoted by  $\mathbf{A}_2$  the in-plane part of the 3-D tensor  $\mathbf{A}$  (i.e.,  $\mathbf{A}_2 = A_{11}\mathbf{c}_1 \otimes \mathbf{c}_1 + A_{12}\mathbf{c}_1 \otimes \mathbf{c}_2 + A_{21}\mathbf{c}_2 \otimes \mathbf{c}_1 + A_{22}\mathbf{c}_2 \otimes \mathbf{c}_2$ ), by  $\mathbf{C}_3 = C_{13}\mathbf{c}_1 \otimes \mathbf{c}_1 + C_{23}\mathbf{c}_2 \otimes \mathbf{c}_2$ , and by  $\mathbf{C}_2\mathbf{A}_2 = (C_{11}A_{11} + C_{12}A_{22})\mathbf{c}_1 \otimes \mathbf{c}_1 + (C_{12}A_{11} + C_{22}A_{22})\mathbf{c}_2 \otimes \mathbf{c}_2 + 4C_{66}A_{12}(\mathbf{c}_1 \otimes \mathbf{c}_2)_S$ . If the material is isotropic, then we obtain the Saint-Venant-Kirchhoff law, i.e., (Voigt notation),

$$\mathbf{C}_2\mathbf{A}_2 = \lambda \text{trace}(\mathbf{A}_2)\mathbf{I}_2 + 2\mu\mathbf{A}_2, \quad \mathbf{C}_3 = \lambda\mathbf{I}_2, \quad C_{33} = \lambda + 2\mu, \quad C_{44} = C_{55} = \mu, \quad (2.6)$$

where  $\lambda = \lambda(\bar{X}, X_3)$  and  $\mu = \mu(\bar{X}, X_3)$  are the Lamé elastic moduli.

We assume further that the material has a weak transversal heterogeneity, i.e.,

$$\hat{\mathbf{C}}_2 = \Sigma\mathcal{O}(\delta), \quad \check{\mathbf{C}}_2 = \frac{1}{12}\bar{\mathbf{C}}_2 + \Sigma\mathcal{O}(\delta), \quad (2.7)$$

$$\hat{\mathbf{C}}_3 = \Sigma\mathcal{O}(\delta), \quad \check{\mathbf{C}}_3 = \frac{1}{12}\bar{\mathbf{C}}_3 + \Sigma\mathcal{O}(\delta), \quad \hat{C}_{33} = \Sigma\mathcal{O}(\delta), \quad \check{C}_{33} = \frac{1}{12}\bar{C}_{33} + \Sigma\mathcal{O}(\delta),$$

where we have denoted by  $\bar{\mathbf{A}}, \hat{\mathbf{A}}, \check{\mathbf{A}}$  the thickness average and first and second-order moment of  $\mathbf{A}$ , i.e.,

$$\bar{\mathbf{A}} = \frac{1}{H} \int_{-H/2}^{H/2} \mathbf{A}(X_3) dX_3, \quad \hat{\mathbf{A}} = \frac{1}{H^2} \int_{-H/2}^{H/2} X_3 \mathbf{A}(X_3) dX_3, \quad \check{\mathbf{A}} = \frac{1}{H^3} \int_{-H/2}^{H/2} X_3^2 \mathbf{A}(X_3) dX_3.$$

For isotropic materials, the condition of weak transversal heterogeneity (2.7) becomes

$$\hat{\lambda} = \Sigma\mathcal{O}(\delta), \quad \hat{\mu} = \Sigma\mathcal{O}(\delta), \quad \check{\lambda} = \frac{1}{12}\bar{\lambda} + \Sigma\mathcal{O}(\delta), \quad \check{\mu} = \frac{1}{12}\bar{\mu} + \Sigma\mathcal{O}(\delta). \quad (2.8)$$

Concerning the pre-stress  $\mathbf{S}^*$ , we assume that the tangential pre-stresses acting on

the surfaces parallel to the mid-surface vanish, i.e.,

$$\mathbf{S}^* = \mathbf{S}_2^* + S_{33}^* \mathbf{c}_3 \otimes \mathbf{c}_3 + \Sigma \mathcal{O}(\delta^2), \quad (2.9)$$

where  $\mathbf{S}_2^*$  is the in-plane pre-stress and  $S_{33}^*$  is the transversal pre-stress.

### 2.3 Moment plate-to-shell equations

We recall here from [18] the moment equations relating the pre-stress  $\mathbf{S}^*$  and the Lagrangian curvature  $\mathbf{K}$ . If

$$\mathbf{M}^* = H^2 \hat{\mathbf{S}}_2^* - \frac{H^2 \hat{S}_{33}^*}{\bar{C}_{33}} \bar{\mathbf{C}}_3,$$

denotes the pre-stress couple, then the shell boundary value problem for the moments reads

$$\operatorname{div}_2 \left( \frac{H^3}{12} \mathcal{M}_2 \mathbf{K} + \mathbf{M}^* \right) = 0 \quad \text{in } \mathcal{S}_0, \quad \left( \frac{H^3}{12} \mathcal{M}_2 \mathbf{K} + \mathbf{M}^* \right) \bar{\boldsymbol{\nu}} = 0 \quad \text{on } \partial \mathcal{S}_0, \quad (2.10)$$

$$\left( \frac{H^3}{12} \mathcal{M}_2 \mathbf{K} + \mathbf{M}^* \right) : \mathbf{K} = 0 \quad \text{in } \mathcal{S}_0. \quad (2.11)$$

In the above,  $\mathcal{M}_2$  denotes the in-plane elastic fourth-order tensor

$$\mathcal{M}_2 \mathbf{A}_2 = \bar{\mathcal{C}}_2 \mathbf{A}_2 - \frac{\bar{\mathbf{C}}_3 : \mathbf{A}_2}{\bar{C}_{33}} \bar{\mathbf{C}}_3$$

which, in the particular case of isotropic materials, becomes

$$\mathcal{M}_2 \mathbf{A}_2 = \frac{2\bar{\mu}\bar{\lambda}}{\bar{\lambda} + 2\bar{\mu}} \operatorname{trace}(\mathbf{A}_2) \mathbf{I}_2 + 2\bar{\mu} \mathbf{A}_2. \quad (2.12)$$

Let us note that the equations and boundary conditions (2.10-2.11) are satisfied if

$$\mathbf{M}^* = -\frac{H^3}{12} \mathcal{M}_2 \mathbf{K} \quad \text{in } \mathcal{S}_0, \quad (2.13)$$

but this is only a sufficient condition for (2.10)-(2.11) and not a necessary one. In the particular case of isotropic materials, from (2.13) we obtain a simple formula relating the invariants of pre-stress moment  $\mathbf{M}^*$  to the invariants of Lagrangian curvature tensor  $\mathbf{K}$ :

$$\operatorname{trace}(\mathbf{M}^*) = -\frac{H^3}{6} \left( \frac{2\bar{\mu}\bar{\lambda}}{\bar{\lambda} + \bar{\mu}} + \bar{\mu} \right) \operatorname{trace}(\mathbf{K}), \quad |(\mathbf{M}^*)^D| = \frac{H^3}{6} \bar{\mu} |(\mathbf{K})^D|, \quad (2.14)$$

where  $(\mathbf{A})^D = \mathbf{A} - \frac{\text{trace}(\mathbf{A})}{2} \mathbf{I}_2$  denotes the two-dimensional deviatoric part of  $\mathbf{A}$ .

### 3 Designing a pre-stressed plate-strip for a given shell-strip

For several common mid-surfaces the small-strain assumption (2.4) drastically reduces the surface width with respect to the curvature radius and this is the main limitation in applying the above plate-to-shell model. This is why, in this section, we introduce another type of shell, called a strip-shell, for which assumption (2.4) can be fulfilled by an appropriate choice of an additional geometric parameter, namely the strip width  $2d$ . From a geometric point of view, a shell-strip has two length scales linking the mid-surface curvature to the strip width and to the shell thickness  $h$ . We prove that the small-strain assumption (2.4) can be satisfied by designing the planar strip and choosing the ratio  $h/d = \mathcal{O}(\sqrt{\delta})$ . Then, we can use the plate-to-shell model described above to obtain the distribution of pre-stress moment  $\mathbf{M}^*$ .

#### 3.1 Designing strips with small strain

The main objective of this section is to design an Eulerian surface-strip  $\mathbf{s}_0$  of a given surface  $\mathcal{U}$  along a given curve  $\mathbf{c} \subset \mathcal{U}$  and a Lagrangian planar strip  $\mathcal{S}_0$  such that the small-strain assumption (2.4) holds.

##### 3.1.1 Constructing a second-order strip along a curve on a surface

Let  $\mathcal{U} \subset \mathbb{R}^3$  be a surface given by its parametric description  $u \rightarrow \mathbf{r}_{\mathcal{U}}(u) \in \mathbb{R}^3$ , where  $u = (u_1, u_2)$  are coordinates in some subset  $\Omega \subset \mathbb{R}^2$ . We denote  $\mathbf{b}_1, \mathbf{b}_2$  for the covariant basic vectors,  $\mathbf{b}^1, \mathbf{b}^2$  for the contravariant basic vectors,  $g_{\alpha\beta} = \mathbf{b}_\alpha \cdot \mathbf{b}_\beta$  for the covariant metric tensor and  $g^{\alpha\beta}$  for the components of its inverse, the contravariant metric tensor. Let  $\mathbf{e}_3 = \mathbf{b}_1 \wedge \mathbf{b}_2 / \sqrt{g_{11}g_{22}}$  be the unit normal vector on  $\mathcal{U}$  and let  $\mathcal{K} = \partial_{u_i} \mathbf{e}_3 \otimes \mathbf{b}^i$  be the curvature tensor.

On the surface  $\mathcal{U}$ , we consider a support curve  $\mathbf{c} \subset \mathcal{U}$  given by the parametric description  $s \rightarrow \mathbf{r}_0(s) = \mathbf{r}_{\mathcal{U}}(u^0(s)) \in \mathcal{U}$  (here  $s \in (0, l)$  is the arc-length) and we denote by  $\mathbf{n}_0$  and  $\mathbf{m}_0$  the normal and binormal unit vectors (see Figure 1).

Let define now the second order strip  $\mathbf{s}_0 \subset \mathcal{U}$  along the curve  $\mathbf{c}$

$$\mathbf{s}_0 = \{\mathbf{r}_{\mathcal{U}}(u(s, q)) ; u(s, q) = u^0(s) + qv^0(s) + \frac{q^2}{2}w^0(s), s \in (0, l), q \in (-d(s), d(s))\}, \quad (3.1)$$

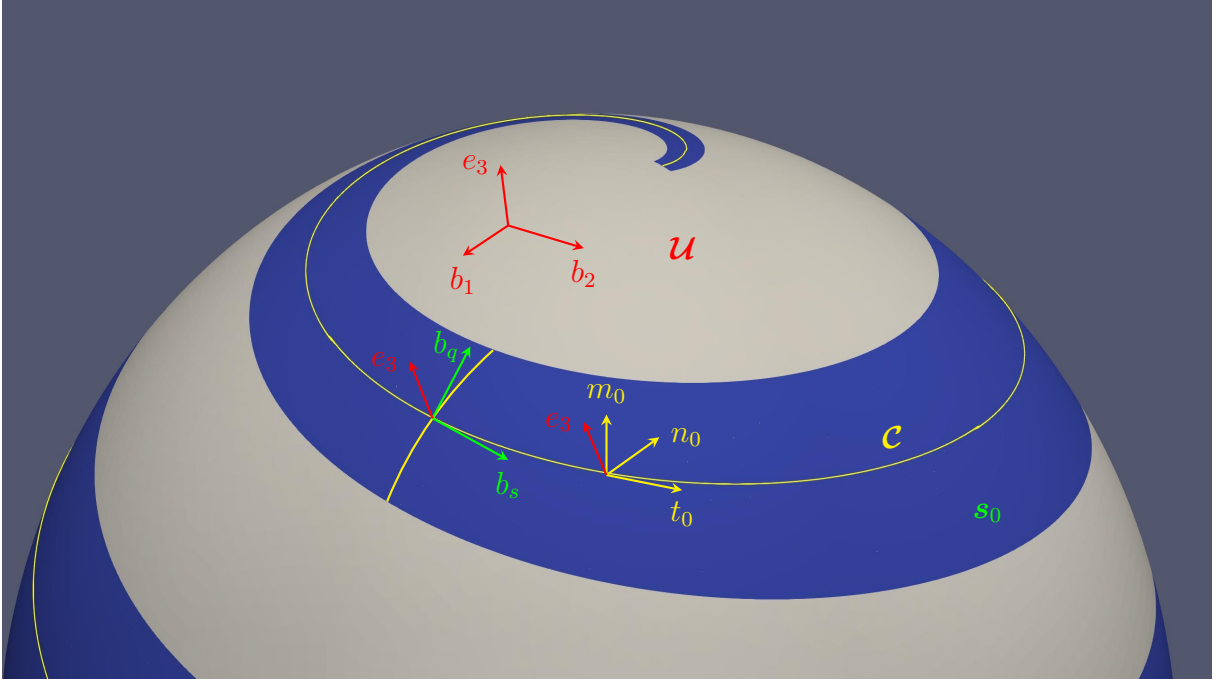


Figure 1: Illustration of a strip  $\mathbf{s}_0$  (with the local basis  $\{\mathbf{b}_s, \mathbf{b}_q, \mathbf{e}_3\}$ ) along a curve  $\mathbf{c}$  (with the local basis  $\{\mathbf{t}_0, \mathbf{n}_0, \mathbf{m}_0\}$  in yellow) belonging to a surface  $\mathcal{U}$  (with the local basis  $\{\mathbf{b}_1, \mathbf{b}_2, \mathbf{e}_3\}$  in red).

where  $2d(s)$  denotes the strip and  $s \rightarrow v^0(s)$  and  $s \rightarrow w^0(s)$  are given by

$$v_i^0(s) = (\mathbf{e}_3(u^0(s)) \wedge \mathbf{t}_0(s)) \cdot \mathbf{b}^i(u^0(s)), \quad w_i^0(s) = -\frac{1}{2} g^{im}(u^0(s)) \frac{\partial g_{ml}}{\partial u_k}(u^0(s)) v_k^0(s) v_l^0(s). \quad (3.2)$$

The couple  $(s, q)$  defines the curvilinear coordinates of the strip-surface  $\mathbf{s}_0$  with the local basis  $\{\mathbf{b}_s, \mathbf{b}_q\}$ , given by  $\mathbf{b}_s = \partial_s \mathbf{r}_{\mathcal{U}}(u(s, q))$ ,  $\mathbf{b}_q = \partial_q \mathbf{r}_{\mathcal{U}}(u(s, q))$ , and the metric tensor  $g_{ss} = |\mathbf{b}_s|^2$ ,  $g_{qq} = |\mathbf{b}_q|^2$ ,  $g_{sq} = \mathbf{b}_s \cdot \mathbf{b}_q$ .

Let  $\eta \ll 1$  be a small parameter, and let

$$k_0^{geo}(s) = k_0(s) \mathbf{e}_3(u^0(s)) \cdot \mathbf{m}_0(s) \quad (3.3)$$

denote the *geodesic curvature* of the curve  $\mathbf{c}$  on surface  $\mathbf{s}_0$  (see for instance [30], chapter 4). One can prove (see Appendix) that if

$$\frac{d(s)}{l} = \mathcal{O}(\eta), \quad d(s) |\mathcal{K}(u^0(s))| = \mathcal{O}(\eta), \quad d(s) k_0^{geo}(s) = \mathcal{O}(\eta), \quad (3.4)$$

then  $\mathbf{s}_0$  is a *strip-surface*, i.e., the following estimations hold

$$g_{ss}(s, q) - 1 + 2q k_0^{geo}(s) = \mathcal{O}(\eta^2), \quad g_{qq}(s, q) - 1 = \mathcal{O}(\eta^2), \quad g_{sq}(s, q) = \mathcal{O}(\eta^2). \quad (3.5)$$

In the local basis  $\{\mathbf{b}^s, \mathbf{b}^q\}$  of the strip-surface  $\mathbf{s}_0$ , the components  $\mathcal{K}_{ss} = \mathcal{K}\mathbf{b}_s \cdot \mathbf{b}_s, \mathcal{K}_{qq} = \mathcal{K}\mathbf{b}_q \cdot \mathbf{b}_q, \mathcal{K}_{sq} = \mathcal{K}\mathbf{b}_s \cdot \mathbf{b}_q$  of curvature tensor  $\mathcal{K}$  can be estimated (at first order with respect to  $\eta$ ) as  $\mathcal{K}_{ss} = \mathcal{K}_{ss}^0 + q\mathcal{K}_{ss}^1 + |\mathcal{K}|\mathcal{O}(\eta^2), \mathcal{K}_{qq} = \mathcal{K}_{qq}^0 + q\mathcal{K}_{qq}^1 + |\mathcal{K}|\mathcal{O}(\eta^2), \mathcal{K}_{sq} = \mathcal{K}_{sq}^0 + q\mathcal{K}_{sq}^1 + |\mathcal{K}|\mathcal{O}(\eta^2)$  where

$$\mathcal{K}_{ss}^0 = \mathcal{K}_{ij}\dot{u}_i^0\dot{u}_j^0, \quad \mathcal{K}_{qq}^0 = \mathcal{K}_{ij}v_i^0v_j^0, \quad \mathcal{K}_{sq}^0 = \mathcal{K}_{ij}\dot{u}_i^0v_j^0, \quad (3.6)$$

$$\mathcal{K}_{ss}^1 = 2\mathcal{K}_{ij}\dot{v}_j^0\dot{u}_j^0, \quad \mathcal{K}_{qq}^1 = 2\mathcal{K}_{ij}w_j^0v_j^0, \quad \mathcal{K}_{sq}^1 = \mathcal{K}_{ij}(\dot{v}_i^0v_j^0 + \dot{u}_i^0w_j^0). \quad (3.7)$$

### 3.1.2 Lagrangian planar strip

Let us consider a planar curve  $\mathcal{C} \subset \mathbb{R}^2$  given by its parametric description  $S \rightarrow \mathbf{R}_0(S) \in \mathbb{R}^2$  and let  $\mathbf{T}_0 = \frac{d}{dS}\mathbf{R}_0$  be the tangent vector of the curve  $\mathcal{C}$ . We suppose that  $S \in (0, L)$  is the arc-length, hence  $|\mathbf{T}_0| = 1$  and  $L$  is the length of the curve  $\mathcal{C}$ . We denote by  $\mathbf{N}_0$  and  $K_0$  the unit normal and the curvature of  $\mathcal{C}$  and let

$$\mathcal{S}_0 = \{\mathbf{R}(S, Q) = \mathbf{R}_0(S) + Q\mathbf{N}_0(S); S \in (0, L), Q \in (-D(S), D(S))\}, \quad (3.8)$$

be the planar strip along  $\mathcal{C}$  where  $2D(S)$  is the (local) strip width. The local basis  $\{\mathbf{b}_S, \mathbf{b}_Q\}$  is given by  $\mathbf{b}_S = \frac{\partial}{\partial S}\mathbf{R} = \mathbf{T}_0 + Q\frac{d}{dS}\mathbf{N}_0, \mathbf{b}_Q = \frac{\partial}{\partial Q}\mathbf{R} = \mathbf{N}_0$ , and from the Frenet formula the metric tensor becomes

$$L_S^2 = g_{SS} = 1 - 2QK_0 + Q^2K_0^2, \quad g_{SQ} = 0, \quad L_Q^2 = g_{QQ} = 1, \quad (3.9)$$

where  $L_S, L_Q$  are the Lamé coefficients. The physical basis will be denoted by  $\mathbf{e}_S = \mathbf{b}_S/L_S, \mathbf{e}_Q = \mathbf{b}_Q$ . Since  $K_0 = K_0^{geo}$ , we see that  $\mathcal{S}_0$  is a strip-surface (i.e., (3.5) holds) if and only if

$$\frac{D(S)}{L} = \mathcal{O}(\eta), \quad D(S)K_0(S) = \mathcal{O}(\eta), \quad \text{for all } S \in (0, L). \quad (3.10)$$

### 3.1.3 Mapping a planar-strip into a surface-strip

Let  $\mathbf{x}_0 : \mathcal{S}_0 \rightarrow \mathbf{s}_0$  be the transformation of the Lagrangian planar strip  $\mathcal{S}_0$  into the Eulerian strip-surface  $\mathbf{s}_0$  given through the parametric transformation

$$s = S, \quad q = Q, \quad l = L, \quad d = D. \quad (3.11)$$

Then, the gradient  $\mathbf{F}_0$  acting from the plane of the Lagrangian strip to the tangent plane  $\mathcal{T}$  of the surface  $\mathbf{s}_0$ , is given by  $\mathbf{F}_0 = \mathbf{b}_s \otimes \mathbf{b}^S + \mathbf{b}_q \otimes \mathbf{b}^Q$ , and from (3.5), (3.9) and (3.10)



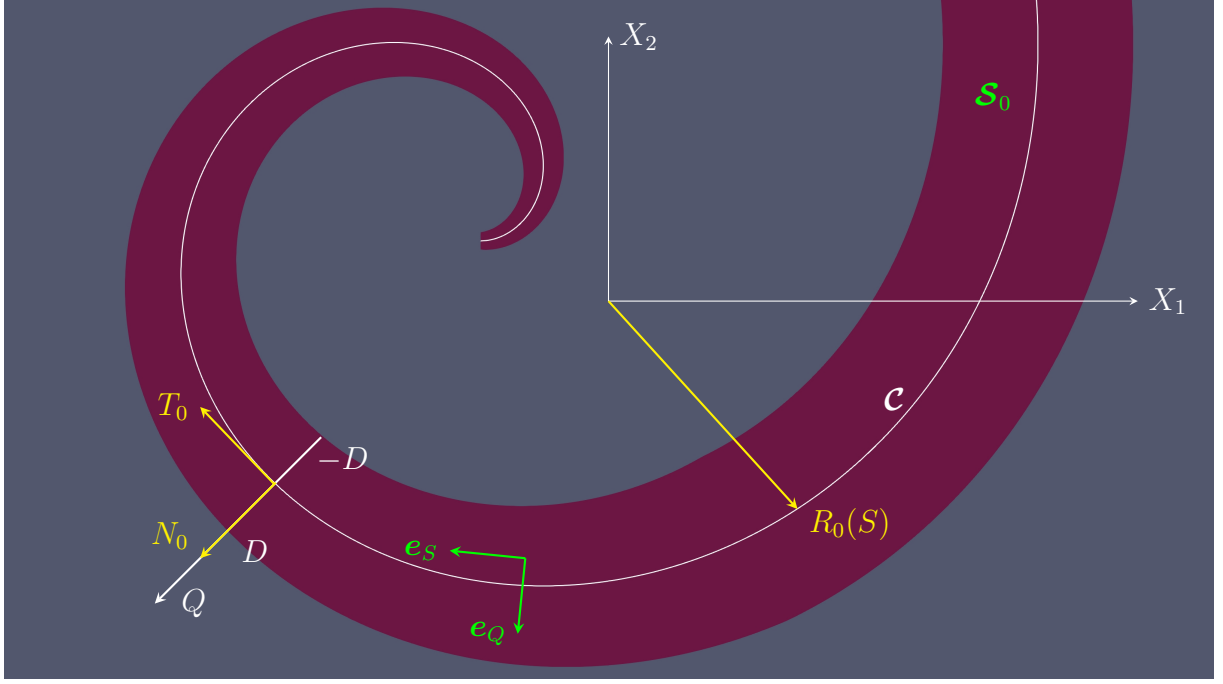


Figure 2: Schematic representation of the Lagrangian planar strip  $\mathcal{S}_0$  (with the local basis  $\{\mathbf{e}_S, \mathbf{e}_Q\}$ ) along a curve  $\mathcal{C}$  (in white) with its local basis  $\{\mathbf{T}_0, \mathbf{N}_0\}$ .

we get  $\mathbf{F}_0^T \mathbf{F}_0 - \mathbf{I}_2 = (1 - g_{ss}/g_{SS})\mathbf{e}_S \otimes \mathbf{e}_S$ . A straightforward computation gives

$$\mathbf{F}_0^T \mathbf{F}_0 - \mathbf{I}_2 = q(K_0(s) - k_0^{geo}(s))\mathbf{e}_S \otimes \mathbf{e}_S + \mathcal{O}(\eta^2),$$

and we notice that if we impose the following *small-strain curvature condition*

$$K_0(s) = k_0^{geo}(s) + \mathcal{O}(\eta^2) \tag{3.12}$$

which relates the curvature of the Lagrangian curve  $\mathcal{C}$  to the geodesic curvature of the Eulerian curve  $\mathbf{c}$ , then the transformation (3.11) satisfies the small strain (or small membrane-strain) assumption for design (2.4) by choosing  $\delta = \eta^2$ .

Let us notice that the above curvature relation (3.12) arrives in a different framework in differential geometry: the class of "asymptotic curves" on a given surface has to have their curvature equal to the geodesic curvature (see [30]). The context here is quite different, as we deal with two curves, an arbitrary Eulerian one and a plane Lagrangian one.

### 3.1.4 Designing the planar strip

Let us discuss here how to design a Lagrangian planar-strip  $\mathcal{S}_0$  that can be transformed into a given strip-surface  $\mathbf{s}_0$  under small-strains deformation.

Here we note that when the curvature  $K_0$  is given by (3.12), it is straightforward to obtain the planar curve  $\mathcal{C}$ . If  $\Theta(s)$  is such that  $\mathbf{T}_0(s) = \cos(\Theta(s))\mathbf{c}_1 + \sin(\Theta(s))\mathbf{c}_2$ , we obtain

$$\Theta(s) = \Theta_0 + \int_0^s K_0(t) dt, \quad \mathbf{R}_0(s) = \int_0^s \mathbf{T}_0(s) dt, \quad (3.13)$$

which is the parametric description of the support curve  $\mathcal{C}$ .

By choosing the width  $d = D$  such that

$$d(s)K_0(s) = \mathcal{O}(\eta), \quad (3.14)$$

the designed planar-strip  $\mathcal{S}_0$ , given by (3.8), admits a small-strain transformation of order  $\mathcal{O}(\eta^2)$  into the strip-surface  $\mathbf{s}_0$ , i.e., (2.4) holds.

## 3.2 Designing the plate-strip for a given shell-strip

Let  $\mathbf{s}$  be an Eulerian shell-strip constructed (see (2.1)) from a surface-strip  $\mathbf{s}_0$  (see Figure 3) and let the Lagrangian plate-strip  $\mathcal{S}$  be constructed (see (2.2)) from a planar-strip  $\mathcal{S}_0$  with  $h = H(1 + \mathcal{O}(\delta^2))$ . If the planar-strip  $\mathcal{S}_0$  is designed such that (3.12) and (3.14) hold, then the transformation  $\mathbf{x}_0 : \mathcal{S}_0 \rightarrow \mathbf{s}_0$  given by (3.11) has a small-strain deformation (2.4) of order  $\eta^2$ . If we now choose the thickness  $h$  to be of order  $\eta = \sqrt{\delta}$  with respect to the strip width  $d$ , i.e.,

$$\delta = \eta^2, \quad \frac{h}{d} = \mathcal{O}(\eta), \quad (3.15)$$

then from (3.4) we obtain (2.3). This means that if (3.12) and (3.14-3.15) are satisfied, this corresponds precisely to the case of plate-to-shell design theory developed in [18] and briefly presented in the section 2.

The designed pre-stress moment  $\mathbf{M}^*$  can be obtained from (2.13) and from the expression of the Lagrangian curvature  $\mathbf{K}$  given by

$$\mathbf{K} = \frac{\mathcal{K}\mathbf{b}_s \cdot \mathbf{b}_s}{L_S^2} \mathbf{e}_S \otimes \mathbf{e}_S + \frac{\mathcal{K}\mathbf{b}_s \cdot \mathbf{b}_q}{L_S} (\mathbf{e}_Q \otimes \mathbf{e}_S + \mathbf{e}_S \otimes \mathbf{e}_Q) + \mathcal{K}\mathbf{b}_q \cdot \mathbf{b}_q \mathbf{e}_Q \otimes \mathbf{e}_Q. \quad (3.16)$$

One can develop the components of the Lagrangian curvature tensor  $\mathbf{K}$  in the physical basis  $\{\mathbf{e}_S, \mathbf{e}_Q\}$  as  $K_{SS} = K_{SS}^0 + qK_{SS}^1 + |\mathcal{K}|\mathcal{O}(\eta^2)$ ,  $K_{QQ} = K_{QQ}^0 + qK_{QQ}^1 + |\mathcal{K}|\mathcal{O}(\eta^2)$ ,

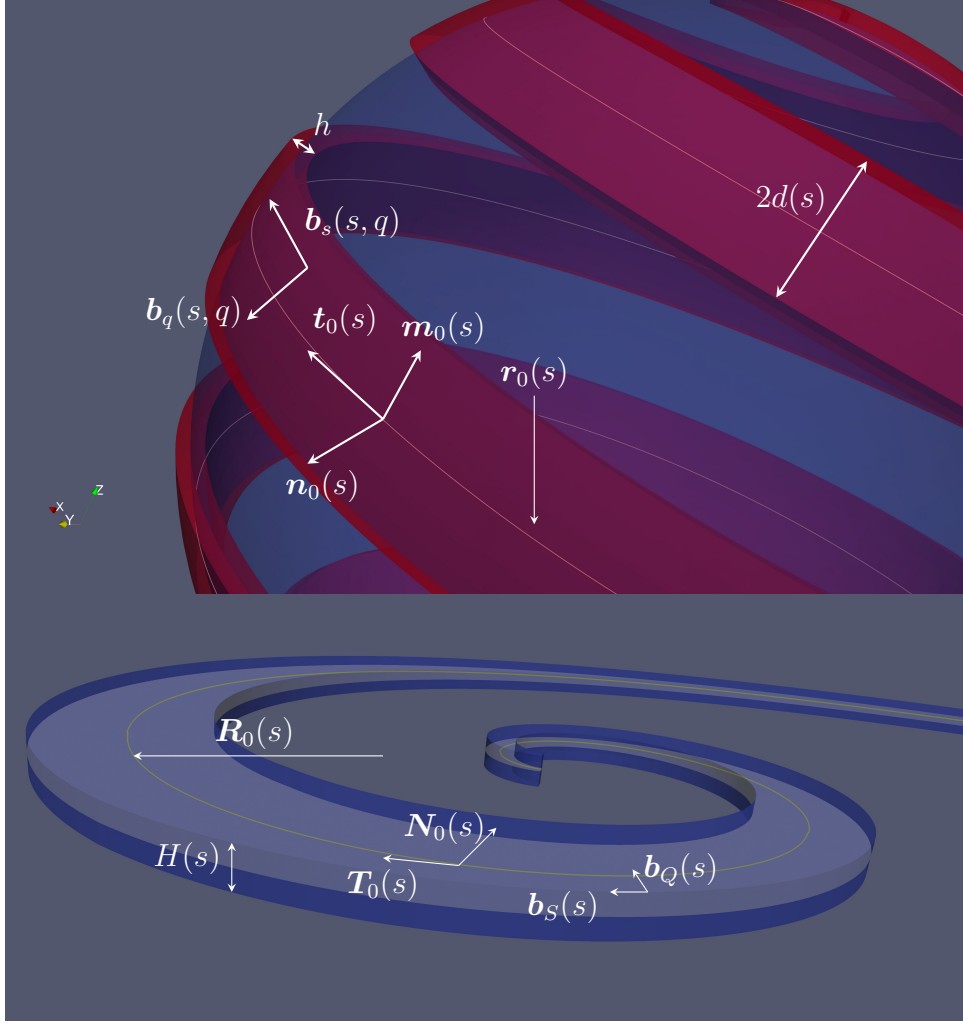


Figure 3: The geometric elements of an Eulerian shell-strip  $\mathbf{s}$  constructed from a mid-surface-strip  $\mathbf{s}_0$  along a support curve  $\mathbf{c}$  (top picture) and the geometric elements of a Lagrangian plate-strip  $\mathbf{S}$  constructed from a planar mid-surface-strip  $\mathbf{S}_0$  along a support curve  $\mathbf{C}$  (bottom picture).

$K_{SQ} = \mathcal{K}_{SQ}^0 + q\mathcal{K}_{SQ}^1 + |\mathcal{K}|\mathcal{O}(\eta^2)$ . Having in mind (3.6)-(3.7), we get:

$$K_{SS}^0 = \mathcal{K}_{ss}^0, \quad K_{SQ}^0 = \mathcal{K}_{sq}^0, \quad K_{QQ}^0 = \mathcal{K}_{qq}^0, \quad (3.17)$$

$$K_{SS}^1 = \mathcal{K}_{ss}^1 + 2K_0, \quad K_{SQ}^1 = \mathcal{K}_{sq}^1 + K_0, \quad K_{QQ}^1 = \mathcal{K}_{qq}^1. \quad (3.18)$$

## 4 Applications to non-developable shells

In this section, we illustrate the plate-to-shell design equations introduced in the previous section, in order to design a sphere and a torus by using only isotropic materials with a weak heterogeneity, i.e., for which (2.6) and (2.8) hold.

## 4.1 Strips on spherical surfaces

Let  $(r, \theta, \varphi)$  be the spherical coordinates in the Eulerian description and denote by  $\mathbf{e}_r = \mathbf{e}_r(\theta, \varphi)$ ,  $\mathbf{e}_\theta = \mathbf{e}_\theta(\theta, \varphi)$ ,  $\mathbf{e}_\varphi = \mathbf{e}_\varphi(\varphi)$  the local physical basis in the Eulerian description. We consider the spherical surface  $\mathcal{U} = \{r = R_*\}$  of radius  $R_*$  with Lamé coefficients  $L_\theta = R_*$ ,  $L_\varphi = R_* \sin(\theta)$  and the unit normal  $\mathbf{e}_3(\theta, \varphi) = \mathbf{e}_r(\theta, \varphi)$ , while the curvature tensor is  $\mathcal{K} = -\frac{1}{R_*} (\mathbf{e}_\theta \otimes \mathbf{e}_\theta + \mathbf{e}_\varphi \otimes \mathbf{e}_\varphi)$ .

On  $\mathcal{U}$  we consider a curve  $\mathbf{c} \subset \mathcal{U}$  given by its parametric description  $s \rightarrow \mathbf{r}_0(s) = R_* \mathbf{e}_r(\theta^0(s), \varphi^0(s)) \in \mathcal{U}$ . The tangent vector is  $\mathbf{t}_0(s) = R_* (\dot{\theta}^0 \mathbf{e}_\theta + \sin(\theta^0) \dot{\varphi}^0 \mathbf{e}_\varphi)$ , and  $s \in (0, l)$  is the arc-length, hence  $\theta^0, \varphi^0$  and  $s$  are related by

$$R_*^2 \left( (\dot{\theta}^0(s))^2 + \sin^2(\theta^0(s)) (\dot{\varphi}^0(s))^2 \right) = 1.$$

A straightforward computation gives  $\mathbf{n}_0^{\mathcal{U}}(s) = \mathbf{e}_r(\theta^0, \varphi^0) \wedge \mathbf{t}_0 = R_* \left( -\sin(\theta^0) \dot{\varphi}^0 \mathbf{e}_\theta + \dot{\theta}^0 \mathbf{e}_\varphi \right)$  so that  $v_\varphi^0 = \dot{\theta}^0 / \sin(\theta^0)$ ,  $v_\theta^0 = -\sin(\theta^0) \dot{\varphi}^0$  and  $w_\varphi^0 = \cot(\theta^0) \dot{\theta}^0 \dot{\varphi}^0$ ,  $w_\theta^0 = 0$  and finally, from (3.2), we can construct (see subsection 3.1.1) the strip-surface  $\mathbf{s}_0$ :

$$\mathbf{s}_0 = \left\{ \varphi = \varphi^0 + q \frac{\dot{\theta}^0}{\sin(\theta^0)} + \frac{q^2}{2} \cot(\theta^0) \dot{\theta}^0 \dot{\varphi}^0, \theta = \theta^0 - q \sin(\theta^0) \dot{\varphi}^0; s \in (0, l), q \in (-d(s), d(s)) \right\}.$$

Then (3.4) reads

$$\frac{d(s)}{R_*} = \mathcal{O}(\eta), \quad d(s) k_0^{geo}(s) = \mathcal{O}(\eta), \quad (4.1)$$

where the geodesic curvature is given by

$$k_0^{geo} = R_*^2 \left( \sin(\theta^0) \dot{\theta}^0 \ddot{\varphi}^0 - [\ddot{\theta}^0 - \sin(\theta^0) \cos(\theta^0) (\dot{\varphi}^0)^2] \sin(\theta^0) \dot{\varphi}^0 + 2(\dot{\theta}^0)^2 \dot{\varphi}^0 \cos(\theta^0) \right). \quad (4.2)$$

Let  $\mathcal{C}$  be the designed planar curve with geodesic curvature  $K_0(s) = k_0^{geo}(s)$  given by the above formula, and let  $\mathcal{S}_0$  be the planar-strip designed on the support Lagrangian curve  $\mathcal{C}$  with the width  $d(s)$  such that (3.14) holds. Then, from the small-strain membrane condition (2.4) we get  $\mathbf{K} = \frac{1}{R_*} (\mathbf{I}_2 + \mathcal{O}(\delta))$ .

To resume, we find that a strip  $\mathbf{s}$  of a spherical shell of radius  $R_*$  along the curve  $\mathbf{c}$ , could be designed from a plate-strip  $\mathcal{S}$  along a curve  $\mathcal{C}$  if (4.1) holds and the Lagrangian curvature  $K_0 = k_0^{geo}$  is given by (4.2). The pre-stress moment in  $\mathcal{S}_0$  is given by  $\mathbf{M}^* = -\frac{H^3}{12R_*} \mathcal{M}_2 \mathbf{I}_2$  and can be obtained with an isotropic and homogeneous pre-stress, i.e.,

$\mathbf{S}_2^* = \sigma^* \mathbf{I}_2$ , where

$$\hat{\sigma}^* = \frac{H}{12R_*}(\bar{C}_{11}^2 + \bar{C}_{12}\bar{C}_{11} - 2\bar{C}_{12}^2)/\bar{C}_{11} = \frac{H}{12R_*} \frac{2\bar{\mu}(3\bar{\lambda} + 2\bar{\mu})}{\bar{\lambda} + 2\bar{\mu}}. \quad (4.3)$$

Here, for simplicity, we used  $\bar{C}_{11} = \bar{\lambda} + 2\bar{\mu}$  and  $\bar{C}_{12} = \bar{\lambda}$ .

#### 4.1.1 "Orange-peeling" strips

In the particular case when  $\ddot{\varphi}^0 = 0$  (i.e.,  $\varphi^0(s) = As + B$ ), the normalization condition reads  $(\dot{\theta}^0)^2(s) + A^2 \sin^2(\theta^0(s)) = 1/R_*^2$ , while the expression of the Lagrangian curvature now has a simpler form. Relations (4.1)-(4.2) become

$$k_0^{geo}(s) = K_0(s) = A \cos \theta^0(s), \quad d(s)A \cos \theta^0(s) = \mathcal{O}(\eta), \quad \frac{d(s)}{R_*} = \mathcal{O}(\eta). \quad (4.4)$$

In Figure 1, we have plotted a spherical strip with the width computed from the above formula  $d(s) = \eta \min\{R_*, \frac{1}{A \cos \theta^0(s)}\}$ , with  $d(s)K_0(s) = d(s)A \cos \theta^0(s)$  in color scale. We note that the strip width has to be drastically reduced when the spherical strip is near the poles.

#### 4.1.2 Covering a sphere with meridian strips

For meridian curves, i.e.,  $\theta^0 = s/R_*$ ,  $\varphi^0 = \text{const}$ , we get  $K_0 = 0$ , hence the designed planar strip is a straight strip with  $d(s) \leq \eta R_*$ . In order to look for conditions that ensure the complete covering of the sphere, we define the meridian strips

$$\mathbf{s}_0^k = \{\varphi = \varphi_k + \frac{q}{\sin(s/R_*)}, \theta = S/R_* + \pi/2; s \in (-\pi R_*/2, \pi R_*/2), q \in (-d(s), d(s))\}.$$

Let  $N^{mer} = [\pi/\eta] + 1$  (we have denoted by  $[x] = \max\{n; n \leq x\}$  the entire part of  $x$ ) be the number of meridians and from the covering condition  $\varphi_k + d(s)/\sin(s/R_*) = \varphi_{k+1} - d(s)/\sin(s/R_*)$ , we obtain

$$\varphi_k = \frac{2\pi}{N^{mer}}k, \quad k = 0, 1, \dots, N^{mer} - 1, \quad d(s) = \frac{\pi R_*}{N^{mer}} \sin(s/R_*).$$

We note that for a small deformation of order of  $\delta = 1\%$  (i.e.,  $\eta = 0.1$ ), we need at least  $N^{mer} = 32$  meridian strips. More precisely, for 32 meridians we obtain an approximation of  $\eta = \pi/32 \approx 0.0981$ ,  $\delta = \pi^2/1024 \approx 0.963\%$  (see Figure 5 for a graphical illustration).

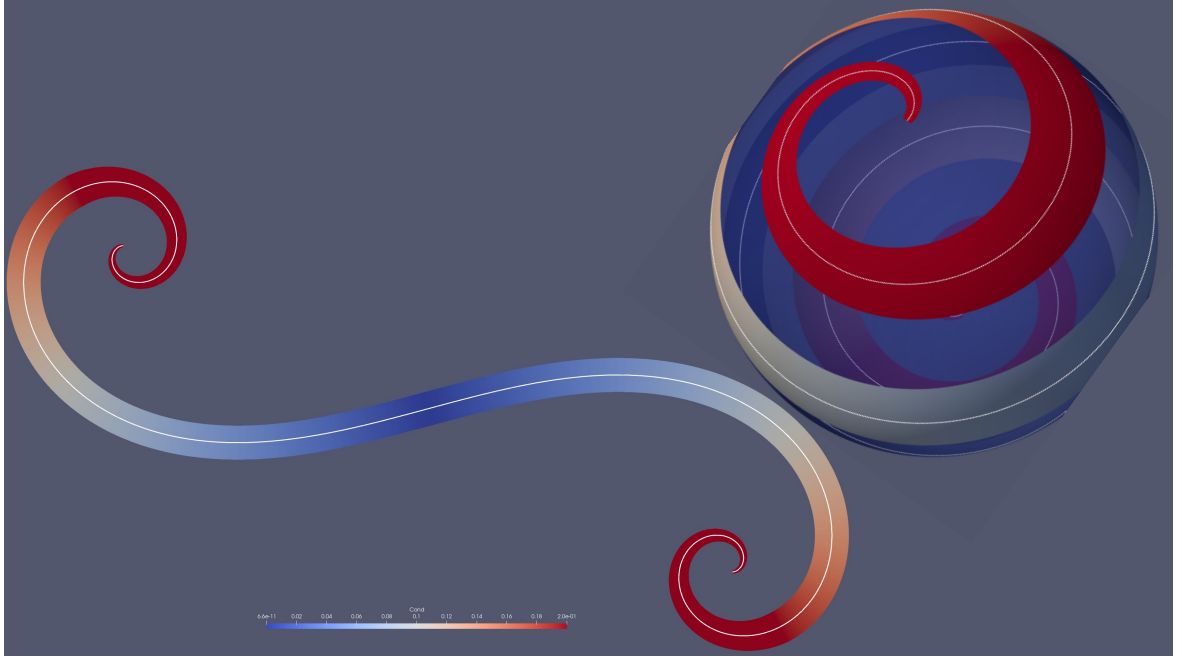


Figure 4: Right: an "orange peeling" spherical strip with  $\ddot{\varphi}^0 = 0$ . Left: the designed planar-strip computed for  $\eta = 0.2, \delta = 4\%$  with  $K_0 d = k_0^{geo} d$  in color scale. The Lagrangian and the Eulerian configurations are plotted at different length scales.

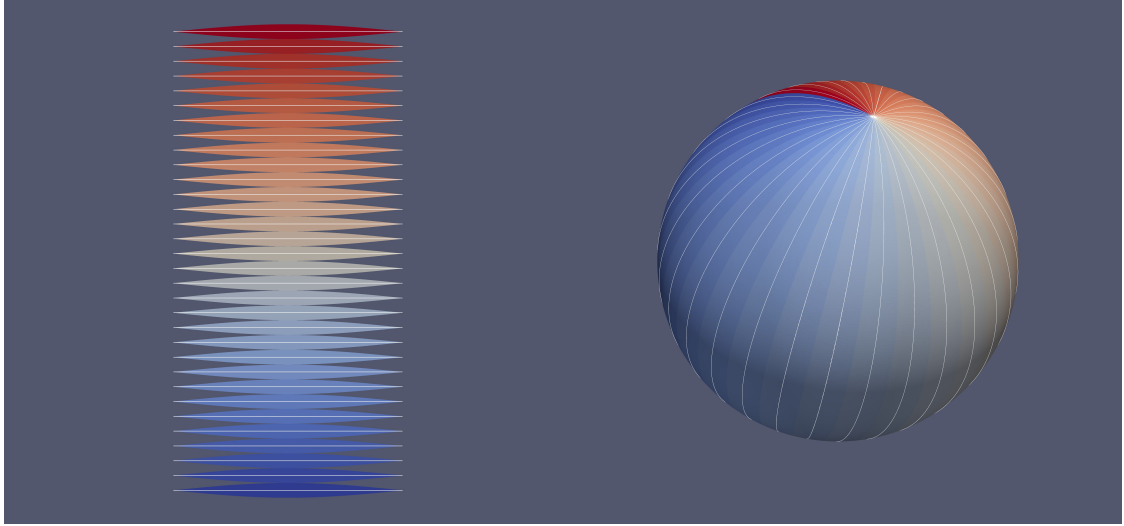


Figure 5: Right: a sphere covered by 32 meridians strips (with strip index in color scale), corresponding to a deformation of  $\delta = 1\%$ . Left: the designed Lagrangian configuration. The Lagrangian and the Eulerian configurations are plotted at different length scales.

### 4.1.3 Covering a sphere with parallel strips

For constant latitude curves, i.e.,  $\theta^0 = \text{const}$ ,  $\varphi^0 = s/(R_* \sin(\theta_0))$ , we have, in addition to (4.1),  $d \cot(\theta^0)/R_* = \mathcal{O}(\eta)$  and  $K_0(s) = \cot(\theta^0)/R_*$ . To design constant latitude strips, let us denote by

$$\mathbf{s}_0^k = \left\{ \varphi = \frac{s}{R_* \cos(\theta_k)} ; \theta = \frac{\pi}{2} - \theta_k - \frac{q}{R_*} ; s \in (-\pi R_* \cos(\theta_k), \pi R_* \cos(\theta_k)), q \in (-d_k, d_k) \right\}$$

and let  $N^{\text{lat}}$  be the number of strips needed to partially cover the sphere, for  $\theta \in (\eta, \pi - \eta)$ . The remaining parts, the spherical callus  $0 < \theta \leq \eta$  and  $\pi - \eta \leq \theta < \pi$  can be covered from a planar disc with small strain (see [18]).

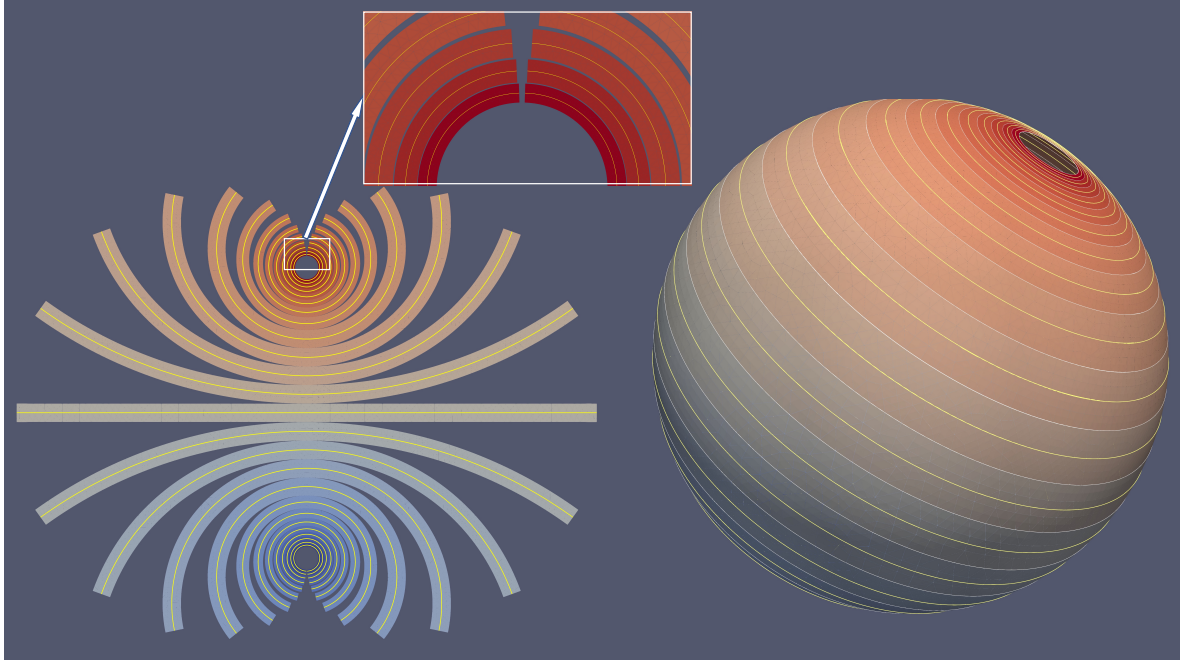


Figure 6: Right: an optimized covering of an almost complete sphere ( $\eta < \theta < \pi - \eta$ ) with 25 parallel strips (with strip index in color scale), corresponding to a deformation of  $\eta^2 = \delta = 1\%$ . Left: the designed Lagrangian configuration. The strip positions and widths were computed from (4.5-4.6). The Lagrangian and the Eulerian configurations are plotted at different length scales.

For a symmetric solution, let us consider  $N^{\text{lat}} = 2M + 1$ , with  $k = -M, \dots, 0, \dots, M$  and  $\theta_0 = 0, \theta_{-k} = -\theta_k$ . From (4.4) and the covering condition, we obtain the following

recursive system

$$d_k \leq \eta R_* \min\{1, \cot(\theta_k)\}, \quad \theta_{k+1} - \theta_k = \frac{d_k + d_{k+1}}{R_*}.$$

For  $\theta \leq \pi/4$  we can consider constant-width strips

$$\theta_k = 2k\eta, \quad d_k = \eta R_*, \quad \text{for } |k| \leq M_0 = \left[\frac{\pi}{8\eta} - \frac{1}{2}\right] \leq M, \quad (4.5)$$

while for  $k > M_0$ , we have to solve recursively the nonlinear equation  $f(x) = x - \eta \cot(x) = \theta_k + d_k/R_*$  to find  $\theta_{k+1} = f^{-1}(\theta_k + d_k/R_*)$ , i.e.,

$$f(\theta_{k+1}) = \theta_k + \frac{d_k}{R_*}, \quad d_{k+1} = R_*(\theta_{k+1} - \theta_k) - d_k, \quad \text{for } M_0 < |k| \leq M. \quad (4.6)$$

The strip positions  $\theta_k$  and strip widths  $d_k$  can be computed from the iterative system (4.5-4.6), while the number of strips  $N^{lat}$  is computed such that  $\theta_M > \pi/2 - \eta$ . In Figure 6, we illustrate the implementation of the above optimal design procedure of a sphere for a given strain  $\delta = 1\%$  ( $\eta = 0.1$ ) corresponding to  $N^{lat} = 25$  strips.

From a technological perspective, the sharp angles between neighbour strips along the vertical line in Figure 6 are very difficult to realize since they are at the lower limit of the photolithography. However, based on a simplified version of the design in Figure 6 we realized in [31] an experimental proof of the design of the sphere.

## 4.2 Strips on a torus

To explore beyond objects with constant curvature, we further discuss the shell-strip covering of the torus. Let  $(r, \varphi, z)$  be the cylindrical coordinates and denote by  $\mathbf{e}_r = \mathbf{e}_r(\varphi)$ ,  $\mathbf{e}_\varphi = \mathbf{e}_\varphi(\varphi)$ ,  $\mathbf{e}_z$  the local physical basis.

We consider the torus  $\mathcal{U}$  with radii  $R_* > r_*$ , given by the parametric description  $(\varphi, \psi) \rightarrow \mathbf{r}_\mathcal{U}(\varphi, \psi) = (R_* + r_* \cos \psi) \mathbf{e}_r(\varphi) + r_* \sin \psi \mathbf{e}_z$ . The local basis is  $\mathbf{b}_\varphi = (R_* + r_* \cos \psi) \mathbf{e}_\varphi$ ,  $\mathbf{b}_\psi = r_* (-\sin \psi \mathbf{e}_r(\varphi) + \cos \psi \mathbf{e}_z)$ , while the Lamé coefficients are  $L_\psi = r_*$ ,  $L_\varphi = R_* + r_* \cos \psi$ . We can compute the physical basis  $\mathbf{e}_\varphi = \mathbf{e}_\varphi(\varphi)$ ,  $\mathbf{e}_\psi = \mathbf{e}_\psi(\varphi, \psi) = -\sin \psi \mathbf{e}_r(\varphi) + \cos \psi \mathbf{e}_z$ , the unit normal  $\mathbf{e}_3(\varphi, \psi) = \cos \psi \mathbf{e}_r(\varphi) + \sin \psi \mathbf{e}_z$  and the curvature tensor

$$\mathcal{K} = -\frac{1}{r_*} \mathbf{e}_\psi \otimes \mathbf{e}_\psi - \frac{\cos \psi}{R_* + r_* \cos \psi} \mathbf{e}_\varphi \otimes \mathbf{e}_\varphi.$$

On  $\mathcal{U}$  we consider a curve  $\mathbf{c} \subset \mathcal{U}$  given by its parametric description  $s \rightarrow \mathbf{r}_0(s) = \mathbf{r}_\mathcal{U}(\varphi^0(s), \psi^0(s)) \in \mathcal{U}$ , where  $s \in (0, l)$  is the arc-length. The tangent vector is  $\mathbf{t}_0(s) =$



$r_*\dot{\psi}^0\mathbf{e}_\psi(\varphi^0, \psi^0) + \dot{\varphi}^0(R_* + r_*\cos\psi^0)\mathbf{e}_\varphi(\varphi^0)$  and  $\varphi^0, \psi^0$ , and  $s$  are related by

$$r_*^2(\dot{\psi}^0(s))^2 + (\dot{\varphi}^0(s))^2(R_* + r_*\cos\psi^0(s))^2 = 1. \quad (4.7)$$

We can now compute

$$\mathbf{n}_0^{\mathcal{U}}(s) = \mathbf{e}_3(\varphi^0, \psi^0) \wedge \mathbf{t}_0 = -r_*\dot{\psi}^0\mathbf{e}_\varphi(\varphi^0) + \dot{\varphi}^0(R_* + r_*\cos\psi^0(s))\mathbf{e}_\psi(\varphi^0(s), \psi^0(s))$$

which gives  $v_\varphi^0 = -r_*\dot{\psi}^0/(R_* + r_*\cos\psi^0)$ ,  $v_\psi^0 = \dot{\varphi}^0(R_* + r_*\cos\psi^0)/r_*$  from (3.2). After some additional computations we get

$$w_\varphi^0 = -r_*\sin\psi^0/(R_* + r_*\cos\psi^0)\dot{\varphi}^0\dot{\psi}^0, \quad w_\psi^0 = 0$$

so that (see subsection 3.1.1) the strip-surface  $\mathbf{s}_0$  is obtained as

$$\mathbf{s}_0 = \{\mathbf{r}\mathbf{u}(\varphi, \psi) ; \varphi = \varphi^0 + qv_\varphi^0 + \frac{q^2}{2}w_\varphi^0, \psi = \psi^0 + qv_\psi^0 ; s \in (0, l), q \in (-d(s), d(s))\}.$$

Let us compute the geodesic curvature: bearing in mind that  $\dot{\mathbf{e}}_\varphi = \dot{\varphi}(\sin\psi\mathbf{e}_\psi - \cos\psi\mathbf{e}_3)$  and  $\dot{\mathbf{e}}_\psi = -\dot{\varphi}\sin\psi\mathbf{e}_\varphi - \dot{\psi}\mathbf{e}_3$ , we get  $\dot{\mathbf{t}}_0(s) = \left(\ddot{\varphi}_0(R_* + r_*\cos\psi_0) - 2\dot{\varphi}_0\dot{\psi}_0r_*\sin\psi_0\right)\mathbf{e}_\varphi + \left(r_*\ddot{\psi}_0 - \dot{\varphi}_0^2(R_* + r_*\cos\psi_0)\right)\mathbf{e}_\psi - \left(r_*\dot{\psi}_0^2 + \dot{\varphi}_0^2(R_* + r_*\cos\psi)\right)\mathbf{e}_3$  and since  $k_0^{geo} = \mathbf{e}_3 \cdot (\mathbf{t}_0 \wedge \dot{\mathbf{t}}_0)$ , we obtain the geodesic curvature as

$$k_0^{geo} = (R_* + r_*\cos\psi_0) \left( r_* (\ddot{\psi}_0\dot{\varphi}_0 - \ddot{\varphi}_0\dot{\psi}_0) + \dot{\varphi}_0^3(R_* + r_*\cos\psi_0)\sin\psi_0 \right) + 2\dot{\varphi}_0\dot{\psi}_0^2r_*^2\sin\psi_0.$$

Then (3.4)-(3.5) reads

$$d(s) \max\left\{\frac{1}{r_*}, \frac{\cos\psi_0(s)}{R_* + r_*\cos\psi_0(s)}\right\} = \mathcal{O}(\eta), \quad d(s)k_0^{geo}(s) = \mathcal{O}(\eta). \quad (4.8)$$

Let  $\mathcal{C}$  be the designed planar curve with the curvature  $K_0(s) = k_0^{geo}(s)$ , given by the above formula, and let the planar-strip  $\mathcal{S}_0$  be designed on the support Lagrangian curve  $\mathcal{C}$  with the width  $d$  such that (4.8) holds. Then the small-strain membrane condition (2.4) holds.

The Lagrangian curvature tensor  $\mathbf{K}$  can be computed from (3.16) and the formulae of the curvature tensor  $\mathcal{K}\mathbf{b}_s \cdot \mathbf{b}_s = \cos\psi(R_* + r_*\cos\psi)(\partial_s\varphi)^2 + r_*(\partial_s\psi)^2$ ,  $\mathcal{K}\mathbf{b}_s \cdot \mathbf{b}_q = \cos\psi(R_* + r_*\cos\psi)\partial_s\varphi\partial_q\varphi + r_*\partial_s\psi\partial_q\psi$ ,  $\mathcal{K}\mathbf{b}_q \cdot \mathbf{b}_q = \cos\psi(R_* + r_*\cos\psi)(\partial_q\varphi)^2 + r_*(\partial_q\psi)^2$ .

Now using (3.17), we get at order  $\eta^0$ :

$$K_{SS}^0 = -\frac{1}{r_*} + \frac{\dot{\varphi}_0^2(R_* + r_* \cos \psi)R_*}{r_*}, \quad K_{QQ}^0 = -\frac{1}{r_*} + \frac{\dot{\psi}_0^2 R_* r_*}{R_* + r_* \cos \psi}, \quad K_{SQ}^0 = \dot{\varphi}_0 \dot{\psi}_0 R_*.$$

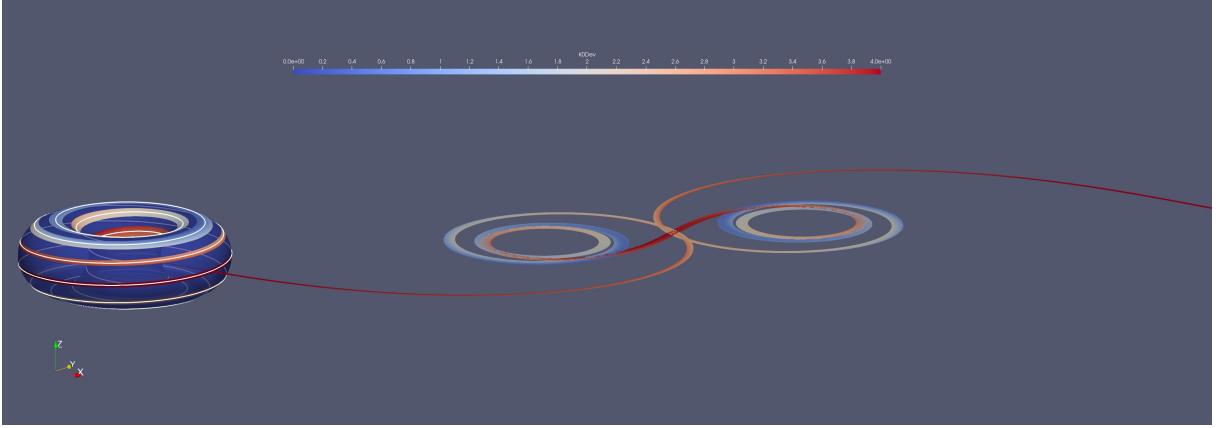


Figure 7: The Eulerian (left) and Lagrangian (right) descriptions of a closed parallel strip on a torus with the width  $d$  given by (4.8) for  $\eta^2 = \delta = 1\%$  (with  $|\mathbf{K}^D|$  in color scale).

In Figures 7 and 8, we have plotted two closed strips on a torus of radii  $R_* = 1, r_* = 0.5$  constructed along two closed curves given in the parametric form as  $t \rightarrow (\varphi^0(t), \psi^0(t))$ , where  $s \rightarrow t(s)$  is obtained from the normalization equation (4.7), and  $t \in [0, 2\pi]$ .

The first one, following the torus' parallels, is given by  $\varphi^0(t) = \alpha t, \psi^0(t) = t$ , with  $\alpha = 10$ . Since the width  $d$  was computed from (4.8), we note that the geodesic curvature  $k_0^{geo}$  was much smaller than the surface curvature  $|\mathcal{K}|$ , which gives an almost uniform width. As we can see from Figure 7, the curvature deviator is very large in the central part, which means that the required pre-stress is not isotropic.

The second one, following the torus' meridians, is given by  $\varphi^0(t) = t, \psi^0(t) = \alpha t$ , with  $\alpha = 20$  (see Figure 8). As before, the width  $d$  computed from (4.8), is almost uniform. The geodesic curvature  $k_0^{geo}$  is rather small, which gives an overall line segment shape of the Lagrangian configuration. However, the Lagrangian curve has periodic oscillations. If we zoom on one period, we note that the curvature deviator is very large, which means that the required pre-stress is again not isotropic. Moreover, the obtained design shows self-intersections which from a practical point of view the technological realization are problematic. This issue, related to local minima along the relaxation path will be the subject of future research.

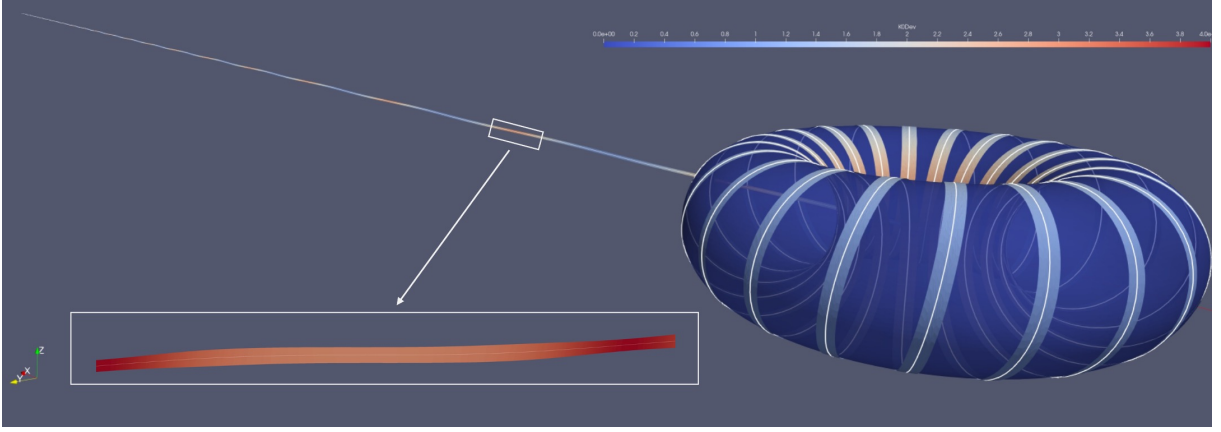


Figure 8: The Eulerian and Lagrangian descriptions of a closed meridian strip on a torus with the width  $d$  given by (4.8) for  $\eta^2 = \delta = 1\%$  (with  $|K^D|$  in color scale). Left bottom: zoom on segment of the Lagrangian description.

### 4.3 Rotoidal strips

Here we construct  $\mathcal{U}$  as a special class of ruled surface  $(s, q) \rightarrow \mathbf{r}(s, q) = \mathbf{r}_0(s) + q\mathbf{v}(s)$ . The curve  $\mathbf{c} \subset \mathbb{R}^3$  is the directrix and  $s \rightarrow \mathbf{v}(s) \in \mathbb{R}^3$  is the direction of the generators which will be supposed to be orthogonal on  $\mathbf{c}$  and described by the rotational angle  $s \rightarrow \theta(s)$ . As previously,  $s \in (0, l)$  is the arc-length,  $\mathbf{t}_0(s), \mathbf{n}_0(s), \mathbf{m}_0(s)$  are the tangent, the normal and the binormal unit vectors, and  $k_0(s), \tau_0(s)$  are the curvature and the torsion of the curve  $\mathbf{c}$ . Let  $\mathbf{v}(s) = \cos(\theta(s))\mathbf{m}_0(s) + \sin(\theta(s))\mathbf{n}_0(s)$  and let  $\mathcal{U} \subset \mathbb{R}^3$  be given by its parametric description  $\mathcal{U} = \{\mathbf{r}(s, q) ; s \in (0, l), q \in (-d_0(s), d_0(s))\}$ , where

$$\mathbf{r}(s, q) = \mathbf{r}_0(s) + q[\cos(\theta(s))\mathbf{m}_0(s) + \sin(\theta(s))\mathbf{n}_0(s)],$$

$d_0$  is the width of  $\mathcal{U}$  and  $\theta(s)$  is the angle between  $\mathbf{m}_0(s)$  and the tangent plane to  $\mathcal{U}$  in  $s$ . Obviously, the couple  $(s, q)$  are orthogonal curvilinear coordinates of  $\mathcal{U}$ , the local basis is given by  $\mathbf{b}_s = (1 - qk_0 \sin(\theta))\mathbf{t}_0 + q(\theta' - \tau_0)[\cos(\theta)\mathbf{n}_0 - \sin(\theta)\mathbf{m}_0]$ ,  $\mathbf{b}_q = \cos(\theta)\mathbf{n}_0 + \sin(\theta)\mathbf{m}_0$  and the metric tensor is  $L_s^2 = g_{ss}(s, q) = (1 - qk_0 \sin(\theta))^2 + q^2(\dot{\theta} - \tau_0)^2$ ,  $g_{sq} = 0$ ,  $L_q^2 = g_{qq} = 1$ . Then, the physical base is  $\mathbf{e}_s = \frac{1}{L_s}\mathbf{b}_s$ ,  $\mathbf{e}_q = \mathbf{b}_q$  and the normal unit vector is given by

$$\mathbf{e}_3(s, q) = \frac{1}{L_s}\mathbf{b}_s \wedge \mathbf{b}_q = \frac{1}{L_s} \left( q(\dot{\theta} - \tau_0)\mathbf{t}_0 + (1 - qk_0 \sin(\theta))[-\cos(\theta)\mathbf{n}_0 + \sin(\theta)\mathbf{m}_0] \right).$$

The curvature tensor can now be written as

$$\mathcal{K} = \frac{1}{L_s} \frac{\partial \mathbf{e}_3}{\partial s} \otimes \mathbf{e}_s + \frac{\partial \mathbf{e}_3}{\partial q} \otimes \mathbf{e}_q, \quad (4.9)$$

and the geodesic curvature of the curve  $\mathbf{c}$  on surface  $\mathcal{U}$  has a simple expression:

$$k_0^{geo}(s) = k_0(s) \sin(\theta(s)). \quad (4.10)$$

Since  $\mathcal{U}$  is a ruled surface, one can get (3.5) from a direct estimation of the metric tensor (i.e., we do not need (3.4)). Indeed, if we consider the rotoid strip-surface

$$\mathbf{s}_0 = \{\mathbf{r}(s, q) ; s \in (0, l), q \in (-d(s), d(s))\} \subset \mathcal{U}$$

along the curve  $\mathbf{c}$  but with a smaller width  $d(s) \leq d_0(s)$  such that

$$d(s)|\mathcal{K}| = \mathcal{O}(\eta), \quad d(s)k_0^{geo}(s) = \mathcal{O}(\eta), \quad d(s)(\dot{\theta}(s) - \tau_0(s)) = \mathcal{O}(\eta), \quad (4.11)$$

then (3.5) holds.

#### 4.3.1 Helicoid

Here, let us consider the helicoid, which is the simplest example of rotating a flat ribbon along a curve. For this, let  $\mathbf{c}$  be a straight line in the  $OX_1$  direction and define the helicoid  $\mathcal{U}$  by choosing  $s = S = X_1, q = Q = X_2$ , and  $\mathbf{t}_0 = \mathbf{c}_1, \mathbf{n}_0 = \mathbf{c}_2$  and  $\mathbf{m}_0 = \mathbf{c}_3$  (here  $\mathbf{c}_1, \mathbf{c}_2, \mathbf{c}_3$  the Cartesian basis in the Lagrangian configuration). After some algebra, we obtain  $\mathbf{b}_s = \mathbf{c}_1 + q\dot{\theta}(\cos(\theta)\mathbf{c}_2 - \sin(\theta)\mathbf{c}_3)$ ,  $\mathbf{b}_q = \sin(\theta)\mathbf{c}_2 + \cos(\theta)\mathbf{c}_3$ , and  $L_s^2 = 1 + q^2\dot{\theta}^2$ ,  $\mathbf{e}_3 = \frac{1}{L_s}(q\dot{\theta}\mathbf{c}_1 - \cos(\theta)\mathbf{c}_2 + \sin(\theta)\mathbf{c}_3)$ . Since  $k_0 = k_0^{geo} = 0$ , we have  $\mathbf{c} = \mathcal{C}$  and bearing in mind that

$$\frac{\partial \mathbf{e}_3}{\partial s} \cdot \mathbf{b}_s = \frac{q\ddot{\theta}}{L_s}, \quad \frac{\partial \mathbf{e}_3}{\partial s} \cdot \mathbf{b}_q = \frac{\partial \mathbf{e}_3}{\partial q} \cdot \mathbf{b}_s = \frac{\dot{\theta}}{L_s}, \quad \frac{\partial \mathbf{e}_3}{\partial q} \cdot \mathbf{b}_q = 0,$$

from (4.9) we deduce that the surface-strip width conditions (4.11) read

$$d(s)\dot{\theta}(s) = \mathcal{O}(\eta), \quad d^2(s)\ddot{\theta}(s) = \mathcal{O}(\eta).$$

We can compute the Lagrangian curvature tensor  $\mathbf{K}$  to find

$$\mathbf{K}(X_1, X_2) = \frac{X_2\ddot{\theta}(X_1)}{L_s(X_1, X_2)}\mathbf{c}_1 \otimes \mathbf{c}_1 + \frac{\dot{\theta}(X_1)}{L_s(X_1, X_2)}(\mathbf{c}_2 \otimes \mathbf{c}_1 + \mathbf{c}_1 \otimes \mathbf{c}_2). \quad (4.12)$$

As we can see in Figure 9, for a constant rotating rate  $\omega$ , i.e.,  $\theta(S) = \omega S$ , the Lagrangian curvature tensor  $\mathbf{K}$  and the pre-stress couple given by

$$\mathbf{K}(X_2) = \frac{\omega}{\sqrt{1 + \omega^2 X_2^2}}(\mathbf{c}_2 \otimes \mathbf{c}_1 + \mathbf{c}_1 \otimes \mathbf{c}_2), \quad -\mathbf{M}^* = \frac{H^3 \bar{\mu}}{6}\mathbf{K}(X_2). \quad (4.13)$$

are traceless, inhomogeneous (with respect to the width variable) and anisotropic.

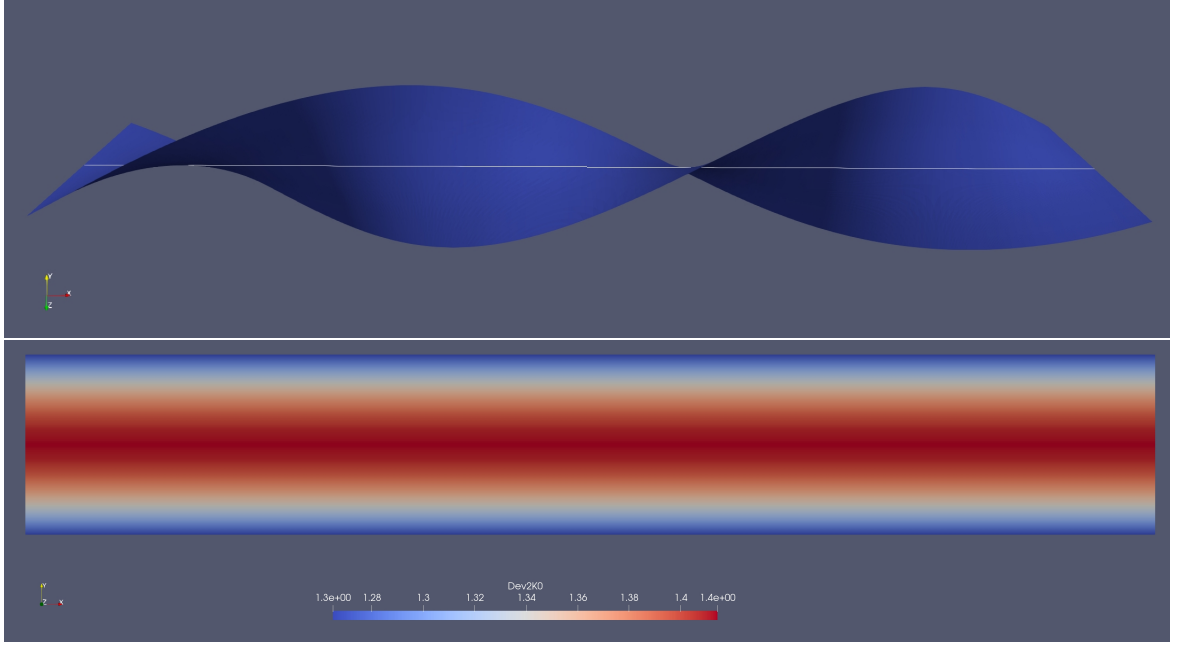


Figure 9: Top: the Eulerian description of a helicoid strip with a constant rotating rate  $\omega$ . Bottom: the Lagrangian description of the strip with the deviator norm  $|K^D|$  in color scale.

We notice that, depending on the rotating rate  $\omega$ , one can approximate

$$\mathbf{K}(X_2) = \frac{\omega}{\sqrt{1 + \omega^2 X_2^2}} (\mathbf{c}_2 \otimes \mathbf{c}_1 + \mathbf{c}_1 \otimes \mathbf{c}_2) \simeq \omega (\mathbf{c}_2 \otimes \mathbf{c}_1 + \mathbf{c}_1 \otimes \mathbf{c}_2)$$

recovering, in the limit of small rotation rate, the result in [32].

#### 4.3.2 Classical Möbius ribbon

Another example of a non-developable surface obtained by rotating a ribbon along a curve is the classical Möbius ribbon, well-documented in the literature. To define it, let  $\mathbf{c}$  be the circle of radius  $R_*$  given by  $\mathbf{r}_0(s) = R_* \mathbf{e}_r(\varphi)$  in the cylindrical coordinates  $r, \varphi, z$  with  $s = R_* \varphi$  and  $s \in (0, 2\pi R_*)$ . Then we have  $\mathbf{t}_0(s) = \mathbf{e}_\varphi(\varphi)$ ,  $\mathbf{n}_0(s) = -\mathbf{e}_r(\varphi)$ ,  $\mathbf{m}_0(s) = \mathbf{e}_z$  and  $k_0(s) = 1/R_*$ ,  $\tau_0(s) = 0$ .

A one-level Möbius ribbon  $\mathcal{U}$  is characterized by the choice  $\theta(s) = \varphi/2 = s/(2R_*)$  but one can also consider any rotating rate  $\omega$  multiple of  $1/2R_*$ . Anyway, we have  $\mathbf{r}(s, q) = R_* \mathbf{e}_r(\varphi) + q[\cos(\varphi/2)\mathbf{e}_z - \sin(\varphi/2)\mathbf{e}_r(\varphi)]$ , with  $q \in (-d_0, d_0)$ , and  $\mathbf{b}_s = (1 - \frac{q}{R_*} \sin(\varphi/2))\mathbf{e}_\varphi - \frac{q}{2R}(\cos(\varphi/2)\mathbf{e}_r + \sin(\varphi/2)\mathbf{e}_z)$ ,  $\mathbf{b}_q = \cos(\varphi/2)\mathbf{e}_z - \sin(\varphi/2)\mathbf{e}_r$ , and we deduce  $L_s^2 = g_{ss}(s, q) = (1 - \frac{q}{R_*} \sin(s/2R_*))^2 + \frac{q^2}{4R_*^2}$ .

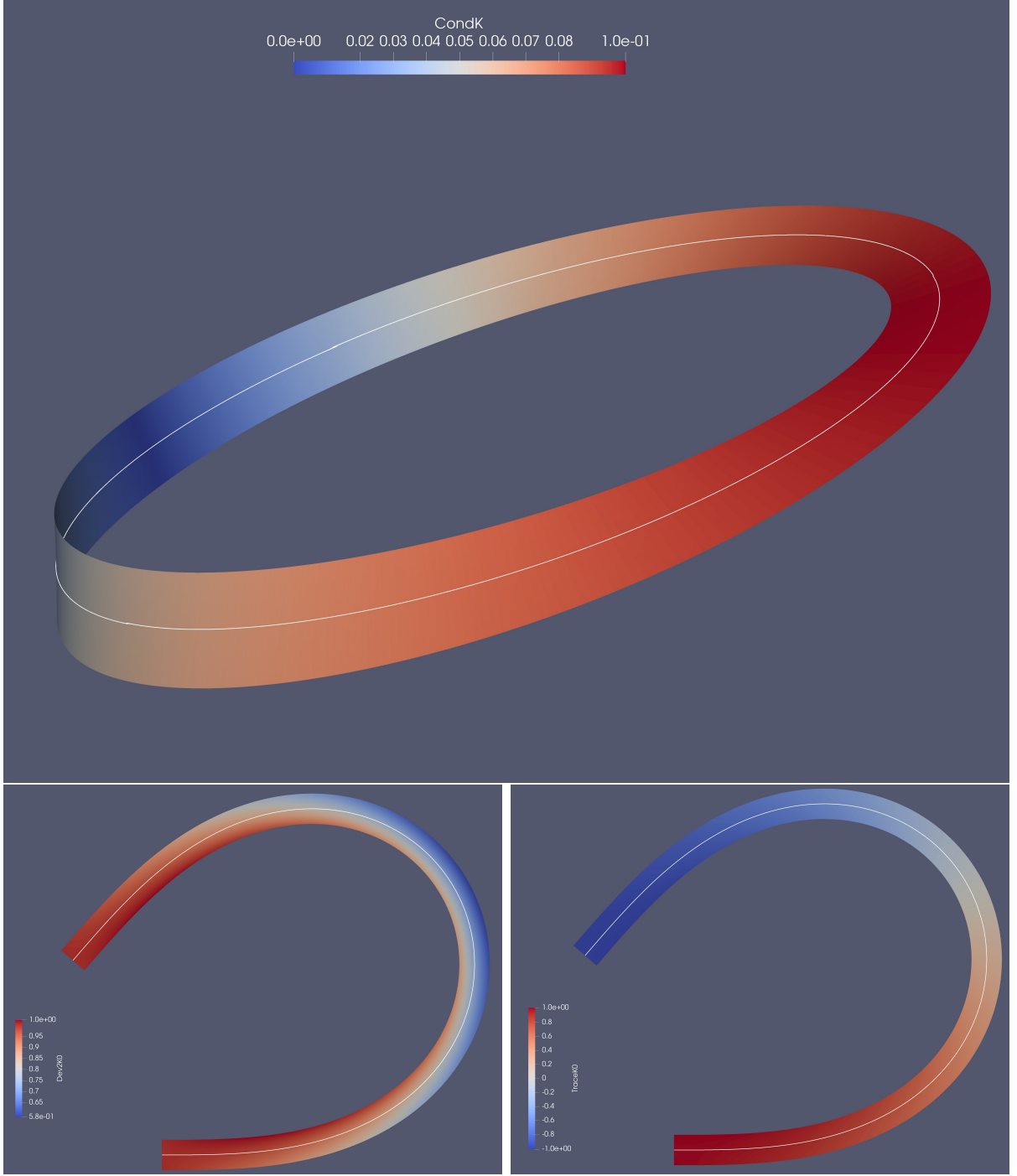


Figure 10: Top: the Eulerian description of the classical Möbius ribbon with  $k_0^{geo}d = K_0d$  in color scale. Bottom: the Lagrangian description of the strip with the deviator norm  $|\mathbf{K}^D|$  in color scale (left) and the curvature  $trace(\mathbf{K})/2$  (right). The Lagrangian and the Eulerian configurations are plotted at different length scales.

Since  $k_0^{geo}(s) = \frac{1}{R_*} \sin(s/2R_*)$ , the surface-strip width conditions (4.11) read

$$\frac{d}{R_*} = \mathcal{O}(\eta), \quad (4.14)$$

and we can construct the Lagrangian curve  $\mathcal{C}$  with the curvature  $K_0(S) = k_0^{geo}(S)$ . A straightforward computation of the Lagrangian curvature tensor gives  $\mathbf{K} = \frac{1}{R_* L_s} (1 + \frac{q^2}{2R_*^2 L_s^2}) \cos(\varphi/2) \mathbf{e}_S \otimes \mathbf{e}_S + \frac{1}{2R_* L_s L_S} (\mathbf{e}_Q \otimes \mathbf{e}_S + \mathbf{e}_S \otimes \mathbf{e}_Q)$ , which can be approximated by

$$R_* \mathbf{K} = \cos(\frac{S}{2R_*}) (1 + Q K_0(S)) \mathbf{e}_S \otimes \mathbf{e}_S + \frac{1 + 2Q K_0(S)}{2} (\mathbf{e}_Q \otimes \mathbf{e}_S + \mathbf{e}_S \otimes \mathbf{e}_Q) + \mathcal{O}(\eta^2).$$

As we can see from Figure 10, the pre-stress associated to the designed Lagrangian strip is neither homogeneous nor isotropic. Moreover, in contrast to the developable Möbius strip, the shape of the Lagrangian strip is not a straight ribbon strip.

## 5 Conclusions and perspectives

The simplest relaxation experiment shows that a uniaxial pre-stressed plate relaxes toward a cylindrical shell. A natural question is then: how to extend this result to a shell of arbitrary curvature? To overcome the geometrical difficulty related to the non-developable nature of an arbitrary shell, in [18] we replaced the isometric transformation (as is the case for cylindrical shells) with small-strains but large rotation transformations of the mid-surfaces. For many applications, the small-strains framework is a technological restriction rather than a mathematical simplification, as we consider small pre-strains and brittle materials. The resulting design model relates the curvature of the target shell shape to the plate shape and the pre-stress distribution.

However, even including small-strains and large rotations, isotropically pre-stressed disks (or squares) relax toward spherical caps (which are non-developable surfaces) only if their radius is small enough [6, 18]. To overcome this geometric restriction, here we consider strip-shells and design arbitrary shells by union of interconnected shell-strips. The local geometric description of an arbitrary shell involves two characteristic lengths and a natural small non-dimensional parameter  $\delta \ll 1$ , which is the product between the thickness of the shell and the curvature norm. The geometries of both plate-strips and shell-strips have an additional characteristic length and thus an additional small parameter  $\eta \ll 1$ , which is the product between the width of the strip and the curvature of its supporting curve. We consider here a special class of strips, called the second-order strips, along an arbitrary curve on the shell mid-surface. These strips have a specific second-order variation with respect to the width variable so that the metric tensor can be estimated with respect to the geodesic curvature of the supporting curve. Moreover, some other additional conditions involving the width have to be fulfilled. Then, for  $\delta = \eta^2$  we

prove here that the small strain condition is fulfilled, thus enabling us to obtain a simple model to design the corresponding plate-strip (i.e., to compute the shape and pre-stress moment of the plate) of any strip of a given shell. More exactly, mapping a plate-strip to a shell-strip naturally introduces the difference between the geodesic curvature of the shell supporting curve and the curvature of the plate supporting curve. By designing the planar supporting curve such that this difference is of order of  $\delta$  we can control the strain to be of order  $\delta$  on all the strip. This relation between the two curvatures is not related to the characterization of the asymptotic curves in differential geometry (see for instance, [30]).

The resulting model was used covers the sphere completely and the torus partially, both of them non-developable surfaces, toward applications in photonics. Regarding the sphere as a union of meridians/parallel strips, the problem is reduced to finding the optimal number and width distribution of each strip in order to fulfill the uniform scaling conditions. For constant latitude strips, the strip width is the solution of an iterative nonlinear system for any given scale  $\delta$ . All these solutions present a common technological drawback, as they rely on very sharp angles (see Figures 5 and 6), difficult to realize by photo-lithography. We notice that at very low length scale ( $nm$ -thick multi layers), as the available technology is only planar, the restriction to homogeneous and isotropic pre-stress is mainly a technological imperative so that an interesting open question concerns all geometries attainable by starting with the pre-stress in this class.

Partial covering of the torus (see Figures 7 and 8), the helicoid (see Figure 9) and the classical Möbius ribbon (see Figure 10) requires non-homogeneous and anisotropic pre-stress, which is very difficult to obtain by using only the planar technology of the epitaxial growth. However, externally unloaded elastic solids can still be endogenously pre-stressed by distributed self-equilibrated force couples as shown in [33, 34, 35, 36] which suggests a way to produce non-isotropic and non-uniform pre-stresses, i.e. including more degrees of freedom to engineer the pre-stress. In that framework, we notice that the weak-transversal heterogeneity assumption may not be fulfilled, so that extending the presented design model to a more general setting may be necessary.

**Acknowledgements.** This work was partially supported by a grant of the French Research Agency (ANR-17-CE24-0027).



## References

- [1] DD Fox, Annie Raoult, and Juan C Simo. A justification of nonlinear properly invariant plate theories. *Archive for rational mechanics and analysis*, 124(2):157–199, 1993.
- [2] Hervé Le Dret and Annie Raoult. The nonlinear membrane model as variational limit of nonlinear three-dimensional elasticity. *Journal de mathématiques pures et appliquées*, 74(6):549–578, 1995.
- [3] Gero Friesecke, Richard D James, and Stefan Müller. A theorem on geometric rigidity and the derivation of nonlinear plate theory from three-dimensional elasticity. *Communications on Pure and Applied Mathematics: A Journal Issued by the Courant Institute of Mathematical Sciences*, 55(11):1461–1506, 2002.
- [4] Gero Friesecke, Stefan Müller, and Richard D James. Rigorous derivation of nonlinear plate theory and geometric rigidity. *Comptes Rendus Mathématique*, 334(2):173–178, 2002.
- [5] Gero Friesecke, Richard D James, and Stefan Müller. A hierarchy of plate models derived from nonlinear elasticity by gamma-convergence. *Archive for rational mechanics and analysis*, 180(2):183–236, 2006.
- [6] Miguel de Benito Delgado and Bernd Schmidt. Energy minimising configurations of pre-strained multilayers. *Journal of Elasticity*, 140:1–33, 2020.
- [7] Fan-Fan Wang, David J Steigmann, and Hui-Hui Dai. On a uniformly-valid asymptotic plate theory. *International Journal of Non-Linear Mechanics*, 112:117–125, 2019.
- [8] de Benito Delgado, Miguel and Schmidt, Bernd. A hierarchy of multilayered plate models. *ESAIM: COCV*, 27:S16, 2021.
- [9] Victor Ya Prinz, Elena V Naumova, Sergey V Golod, Vladimir A Seleznev, Andrey A Bocharov, and Vitaliy V Kubarev. Terahertz metamaterials and systems based on rolled-up 3d elements: designs, technological approaches, and properties. *Scientific reports*, 7:43334, 2017.
- [10] Marta Lewicka, Annie Raoult, and Diego Ricciotti. Plates with incompatible pre-strain of high order. In *Annales de l’Institut Henri Poincaré (C) Non Linear Analysis*, volume 34, pages 1883–1912. Elsevier, 2017.

- [11] Marta Lewicka and Annie Raoult. Thin structures with imposed metric. *ESAIM: Proceedings and Surveys*, 62:79–90, 2018.
- [12] Vladimir Seleznev, Hiroshi Yamaguchi, Yoshiro Hirayama, and Victor Prinz. Single-turn GaAs/InAs nanotubes fabricated using the supercritical CO<sub>2</sub> drying technique. *Japanese journal of applied physics*, 42(7A):L791, 2003.
- [13] V Ya Prinz. A new concept in fabricating building blocks for nanoelectronic and nanomechanic devices. *Microelectronic engineering*, 69(2-4):466–475, 2003.
- [14] V Ya Prinz and SV Golod. Elastic silicon-film-based nanoshells: formation, properties, and applications. *Journal of Applied Mechanics and Technical Physics*, 47(6):867–878, 2006.
- [15] V Ya Prinz, D Grützmacher, A Beyer, C David, B Ketterer, and E Deckardt. A new technique for fabricating three-dimensional micro-and nanostructures of various shapes. *Nanotechnology*, 12(4):399, 2001.
- [16] V Ya Prinz, VA Seleznev, AK Gutakovsky, AV Chehovskiy, VV Preobrazhenskii, MA Putyato, and TA Gavrilova. Free-standing and overgrown ingaas/gaas nanotubes, nanohelices and their arrays. *Physica E: Low-dimensional Systems and Nanostructures*, 6(1-4):828–831, 2000.
- [17] Roger Fosdick and Eliot Fried. *The mechanics of ribbons and Möbius bands*. Springer, 2016.
- [18] Alexandre Danescu and Ioan R Ionescu. Shell design from planar pre-stressed structures. *Mathematics and Mechanics of Solids*, page 1081286520901553, 2020.
- [19] David J Steigmann. Koiter shell theory from the perspective of three-dimensional nonlinear elasticity. *Journal of Elasticity*, 111(1):91–107, 2013.
- [20] Philippe G Ciarlet and Cristinel Mardare. A nonlinear shell model of koiter’s type. *Comptes Rendus Mathématique*, 356(2):227–234, 2018.
- [21] David J Steigmann. Thin-plate theory for large elastic deformations. *International Journal of Non-Linear Mechanics*, 42(2):233–240, 2007.
- [22] David J Steigmann. Asymptotic finite-strain thin-plate theory for elastic solids. *Computers & Mathematics with Applications*, 53(2):287–295, 2007.

- [23] David J Steigmann and Ray W Ogden. Classical plate buckling theory as the small-thickness limit of three-dimensional incremental elasticity. *ZAMM-Journal of Applied Mathematics and Mechanics/Zeitschrift für Angewandte Mathematik und Mechanik*, 94(1-2):7–20, 2014.
- [24] Hillel Aharoni, Eran Sharon, and Raz Kupferman. Geometry of thin nematic elastomer sheets. *Phys. Rev. Lett.*, 113:257801, Dec 2014. doi: 10.1103/PhysRevLett.113.257801.
- [25] Hillel Aharoni, Yu Xia, Xinyue Zhang, Randall D. Kamien, and Shu Yang. Universal inverse design of surfaces with thin nematic elastomer sheets. *Proceedings of the National Academy of Sciences*, 115(28):7206–7211, 2018. ISSN 0027-8424. doi: 10.1073/pnas.1804702115.
- [26] Itay Griniasty, Hillel Aharoni, and Efi Efrati. Curved geometries from planar director fields: Solving the two-dimensional inverse problem. *Phys. Rev. Lett.*, 123:127801, Sep 2019. doi: 10.1103/PhysRevLett.123.127801.
- [27] Wim M. van Rees, Etienne Vouga, and L. Mahadevan. Growth patterns for shape-shifting elastic bilayers. *Proceedings of the National Academy of Sciences*, 114(44):11597–11602, 2017. ISSN 0027-8424. doi: 10.1073/pnas.1709025114.
- [28] A Danescu, C Chevalier, G Grenet, Ph Regreny, X Letartre, and Jean-Louis Leclercq. Spherical curves design for micro-origami using intrinsic stress relaxation. *Applied Physics Letters*, 102(12):123111, 2013.
- [29] A Danescu, Ph Regreny, P Cremillieu, and JL Leclercq. Fabrication of self-rolling geodesic objects and photonic crystal tubes. *Nanotechnology*, 29(28):285301, 2018.
- [30] Michael Spivak. *A comprehensive Introduction to differential geometry*, volume 3. Publish or Perish, 1999.
- [31] Alexandre Danescu, Philippe Regreny, Pierre Cremillieu, Jean-Louis Leclercq, and Ioan R. Ionescu. Covering a surface with pre-stressed ribbons : from theory to nano-structure fabrication. *arXiv preprint 2111.11253*, 2021.
- [32] Shahaf Armon, Efi Efrati, Raz Kupferman, and Eran Sharon. Geometry and mechanics in the opening of chiral seed pods. *Science*, 333(6050):1726–1730, 2011. doi: 10.1126/science.1203874.

- [33] J. William Boley, Wim M. van Rees, Charles Lissandrello, Mark N. Horenstein, Ryan L. Truby, Arda Kotikian, Jennifer A. Lewis, and L. Mahadevan. Shape-shifting structured lattices via multimaterial 4d printing. *Proceedings of the National Academy of Sciences*, 116(42):20856–20862, 2019. ISSN 0027-8424. doi: 10.1073/pnas.1908806116.
- [34] Jungwook Kim, James A. Hanna, Myunghwan Byun, Christian D. Santangelo, and Ryan C. Hayward. Designing responsive buckled surfaces by halftone gel lithography. *Science*, 335(6073):1201–1205, 2012. doi: 10.1126/science.1215309.
- [35] A. S. Gladman, E. A. Matsumoto, R. G. Nuzzo, L. Mahadevan, and J. A. Lewis. Biomimetic 4d printing. *Nature Materials*, 15:413–419, 2016.
- [36] Emmanuel Siéfert, Etienne Reyssat, José Bico, and Benoît Roman. Bio-inspired pneumatic shape-morphing elastomers. *Nature materials*, 18(1):24, 2019.

## 6 Appendix

Here we aim to construct a surface-strip  $\mathbf{s}_0$  of a given surface  $\mathcal{U}$  along a given curve  $\mathbf{c} \subset \mathcal{U}$  such that  $\mathbf{s}_0$  satisfies (3.4)-(3.5). Let us consider a surface  $\mathcal{U} \subset \mathbb{R}^3$  given by its parametric description  $u \rightarrow \mathbf{r}_{\mathcal{U}}(u) \in \mathbb{R}^3$ , where  $u = (u_1, u_2)$  are the parameters belonging to  $\Omega \subset \mathbb{R}^2$ . We denote by  $\mathbf{b}_1 = \partial_{u_1} \mathbf{r}_{\mathcal{U}}$ ,  $\mathbf{b}_2 = \partial_{u_2} \mathbf{r}_{\mathcal{U}}$  the covariant basic vectors and by  $g_{11} = |\mathbf{b}_1|^2$ ,  $g_{22} = |\mathbf{b}_2|^2$ ,  $g_{12} = \mathbf{b}_1 \cdot \mathbf{b}_2$  the covariant fundamental magnitudes of the first order. Let  $\mathcal{T} = \mathcal{T}(u) = Sp\{\mathbf{b}_1, \mathbf{b}_2\}$  be the two-dimensional vector space tangent to the surface  $\mathcal{U}$ . We also denote by  $g = \sqrt{g_{11}g_{22} - g_{12}^2}$  the element of area and by  $\mathbf{e}_3 = \mathbf{b}_1 \wedge \mathbf{b}_2 / g$  the unit normal of  $\mathcal{U}$ . We introduce the contravariant tangent basis, denoted by  $\mathbf{b}^1, \mathbf{b}^2$ , and the contravariant fundamental magnitudes of the first order  $g^{11} = |\mathbf{b}^1|^2 = g_{22}/g^2$ ,  $g^{22} = |\mathbf{b}^2|^2 = g_{11}/g^2$ ,  $g^{12} = \mathbf{b}^1 \cdot \mathbf{b}^2 = -g_{12}/g^2$ .

On this surface, we consider a non-planar curve  $\mathbf{c} \subset \mathcal{U}$  given by its parametric description  $s \rightarrow \mathbf{r}_0(s) = \mathbf{r}_{\mathcal{U}}(u^0(s)) \in \mathcal{U}$ , where  $s \in (0, l)$  is the arc-length. Let  $\mathbf{t}_0(s) = \frac{d}{ds} \mathbf{r}_0(s) = \nabla \mathbf{r}_{\mathcal{U}} \frac{d}{ds} u^0(s) = \frac{d}{ds} u_i^0(s) \mathbf{b}_i(u^0(s)) \in \mathcal{T}(u^0)$  be the tangent unit vector on the curve. We denote by  $\mathbf{n}_0^{\mathcal{U}}(s) = \mathbf{e}_3(u^0(s)) \wedge \mathbf{t}_0(s)$  the unit vector which has the direction of the projection of  $\mathbf{n}_0(s)$  in the plane  $\mathcal{T}(u^0)$ , i.e.,  $\mathbf{n}_0^{\mathcal{U}}(s)$  belongs to the intersection of the normal plane on  $\mathbf{c}$  with the tangent plane of the surface  $\mathcal{U}$ , and  $|\mathbf{n}_0^{\mathcal{U}}(s)| = 1$ ,  $\mathbf{n}_0^{\mathcal{U}}(s) \cdot \mathbf{t}_0(s) = 0$ . From the above Frenet formula we get

$$\frac{d\mathbf{n}_0^{\mathcal{U}}(s)}{ds} \cdot \mathbf{t}_0(s) = -k_0(s)(\mathbf{n}_0(s) \wedge \mathbf{e}_3(u^0(s))) \cdot \mathbf{t}_0(s) = -k_0(s)\mathbf{e}_3(u^0(s)) \cdot \mathbf{m}_0(s) \quad (6.1)$$

and we recognize here *the geodesic curvature*  $k_0^{geo}$  of the curve  $\mathbf{c} \subset \mathcal{U}$ , given by (4.10).

Let  $s \rightarrow v^0(s)$  be such that

$$\mathbf{n}_0^{\mathcal{U}}(s) = \nabla \mathbf{r}_{\mathcal{U}} v^0(s) = v_i^0(s) \mathbf{b}_i(u^0(s)). \quad (6.2)$$

Then we can define the strip  $\mathbf{s}_0 \subset \mathcal{U}$  given by (3.1) where  $2d(s)$  is the strip "width" and  $w^0$  will be determined later. Denoting by  $u_i(s, q) = u_i^0(s) + qv_i^0(s) + \frac{q^2}{2}w_i^0(s)$ , by  $\dot{u}_i(s, q) = \partial_s u_i(s, q) = \dot{u}_i^0(s) + q\dot{v}_i^0(s) + \frac{q^2}{2}\dot{w}_i^0(s)$  and by  $u'_i(s, q) = \partial_q u_i(s, q) = v_i^0(s) + qw_i^0(s)$ , the local basis is given by

$$\mathbf{b}_s(s, q) = \frac{\partial}{\partial s} \mathbf{r}(s, q) = \dot{u}_i(s, q) \mathbf{b}_i(u(s, q)), \quad \mathbf{b}_q(s, q) = \frac{\partial}{\partial q} \mathbf{r}(s, q) = u'_i(s, q) \mathbf{b}_i(u(s, q)),$$

while the metric tensor is given by

$$g_{ss}(s, q) = g_{ij}(u(s, q)) \dot{u}_i(s, q) \dot{u}_j(s, q), \quad g_{sq} = g_{ij}(u(s, q)) \dot{u}_i(s, q) u'_j(s, q), \quad (6.3)$$

$$g_{qq} = g_{ij}(u(s, q)) u'_i(s, q) u'_j(s, q). \quad (6.4)$$

If we suppose now that

$$d(s) \frac{\partial g_{ij}}{\partial u_k}(u^0(s)) = \mathcal{O}(\eta), \quad d^2(s) \frac{\partial^2 g_{ij}}{\partial u_k \partial u_l}(u^0(s)) = \mathcal{O}(\eta^2), \quad (6.5)$$

then we get

$$g_{ij}(u(s, q)) = g_{ij}(u^0(s)) + q \frac{\partial g_{ij}}{\partial u_k}(u^0(s)) v_k^0(s) + \mathcal{O}(\eta^2).$$

This last estimation and the following assumptions

$$d(s) \frac{\partial g_{ij}}{\partial u_k}(u^0(s)) v_k^0(s) \frac{du_i^0}{ds}(s) \frac{du_j^0}{ds}(s) = \mathcal{O}(\eta), \quad \text{for all } s \in (0, s),$$

$$d(s) \frac{\partial g_{ij}}{\partial u_k}(u^0(s)) v_k^0(s) \frac{du_i^0}{ds}(s) v_j^0(s) = \mathcal{O}(\eta), \quad \text{for all } s \in (0, s),$$

$$d(s) \frac{\partial g_{ij}}{\partial u_k}(u^0(s)) v_k^0(s) v_i^0(s) v_j^0(s) = \mathcal{O}(\eta), \quad \text{for all } s \in (0, s),$$

can be used to estimate the metric tensor from (6.3-6.4)

$$g_{ss} = g_{ij}(u^0(s)) \frac{du_i^0}{ds} \frac{du_j^0}{ds} + q \left( 2g_{ij}(u^0(s)) \frac{du_i^0}{ds} \frac{dv_j^0}{ds} + \frac{\partial g_{ij}}{\partial u_k}(u^0(s)) v_k^0 \frac{du_i^0}{ds} \frac{du_j^0}{ds} \right) + \mathcal{O}(\eta^2)$$

$$g_{sq} = g_{ij}(u^0(s)) \frac{du_i^0}{ds} v_j^0 + q \left( g_{ij}(u^0(s)) \frac{dv_i^0}{ds} v_j^0 + g_{ij}(u^0(s)) \frac{du_i^0}{ds} w_j^0 + \frac{\partial g_{ij}}{\partial u_k}(u^0(s)) v_k^0 \frac{du_i^0}{ds} v_j^0 \right) + \mathcal{O}(\eta^2),$$

$$g_{qq} = g_{ij}(u^0(s)) v_i^0 v_j^0 + q \left( 2g_{ij}(u^0(s)) w_i^0 v_j^0 + \frac{\partial g_{ij}}{\partial u_k}(u^0(s)) v_k^0 v_i^0 v_j^0 \right) + \mathcal{O}(\eta^2).$$

We now choose  $w^0$  such that the first order term (i.e., which multiplies  $q$ ) vanishes in expression of  $g_{qq}$ , i.e., we put  $w_0$  given by (3.2). Then, bearing in mind that  $g_{ij} v_i^0 v_j^0 = |\mathbf{n}_0^\mathcal{U}(s)|^2 = 1$  we get

$$g_{qq} = 1 + \mathcal{O}(\eta^2). \quad (6.6)$$

Using (3.2) again, we get

$$g_{ij} \frac{dv_i^0}{ds} v_j^0 + g_{ij} \frac{du_i^0}{ds} w_j^0 + \frac{\partial g_{ij}}{\partial u_k} v_k^0 \frac{du_i^0}{ds} v_j^0 = g_{ij} \frac{dv_i^0}{ds} v_j^0 + \frac{1}{2} \frac{\partial g_{ij}}{\partial u_k} v_k^0 \frac{du_i^0}{ds} v_j^0 = \frac{d\mathbf{n}_0^\mathcal{U}}{ds} \cdot \mathbf{n}_0^\mathcal{U} = 0,$$

hence the first order term vanishes in expression of  $g_{sq}$  and since  $g_{ij} \frac{du_i^0}{ds} v_j^0 = \mathbf{n}_0^\mathcal{U}(s) \cdot \mathbf{t}_0(s) = 0$  we get

$$g_{sq} = \mathcal{O}(\eta^2). \quad (6.7)$$

If we note that

$$g_{ij} \frac{du_i^0}{ds} \frac{du_j^0}{ds} = |\mathbf{t}_0|^2 = 1, \quad 2g_{ij} \frac{du_i^0}{ds} \frac{dv_i^0}{ds} + \frac{\partial g_{ij}}{\partial u_k} v_k^0 \frac{du_i^0}{ds} \frac{du_j^0}{ds} = 2 \frac{d\mathbf{n}_0^\mathcal{U}}{ds} \cdot \mathbf{t}_0,$$

we obtain

$$g_{ss}(s, q) = 1 - 2qk_0(s) \mathbf{e}_3(u^0(s)) \cdot \mathbf{m}_0(s) + \mathcal{O}(\eta^2). \quad (6.8)$$

From (6.6-6.8) we conclude that if (3.4) holds, then subsurface  $\mathbf{s}_0$  of  $\mathcal{U}$ , given by (3.1), is a strip-surface, i.e., (3.5) holds.